![ktu 1922]

Kaunas University of Technology

Faculty of Chemical Technology

Experimental Investigation of an Innovative Complex Air Cleaner Efficiency

Master's Final Degree Project

Vivian Achao Surgelas

Project author

Chief Researcher dr. Tadas Prasauskas

Supervisor

Kaunas, 2023

Kaunas University of Technology

Faculty of Chemical Technology

Experimental Investigation of an Innovative Complex Air Cleaner Efficiency
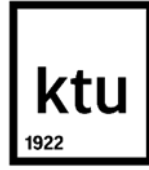
Master's Final Degree Project

Environmental Engineering (6211EX003)

Vivian Achao Surgelas

Project author

Chief Researcher dr. Tadas Prasauskas

Supervisor

Prof. Dainius Martuzevičius

Reviewer

Kaunas, 2023

Kaunas University of Technology

Faculty of Chemical Technology

Vivian Achao Surgelas

Experimental Investigation of an Innovative Complex Air Cleaner Efficiency

Declaration of Academic Integrity

I confirm the following:

1. I have prepared the final degree project independently and honestly without any violations of the copyrights or other rights of others, following the provisions of the Law on Copyrights and Related Rights of the Republic of Lithuania, the Regulations on the Management and Transfer of Intellectual Property of Kaunas University of Technology (hereinafter – University) and the ethical requirements stipulated by the Code of Academic Ethics of the University;

2. All the data and research results provided in the final degree project are correct and obtained legally; none of the parts of this project are plagiarised from any printed or electronic sources; all the quotations and references provided in the text of the final degree project are indicated in the list of references;

3. I have not paid anyone any monetary funds for the final degree project or the parts thereof unless required by the law;

4. I understand that in the case of any discovery of the fact of dishonesty or violation of any rights of others, the academic penalties will be imposed on me under the procedure applied at the University; I will be expelled from the University and my final degree project can be submitted to the Office of the Ombudsperson for Academic Ethics and Procedures in the examination of a possible violation of academic ethics.

<div align="right">

Vivian Achao Surgelas
Confirmed electronically

</div>

Summary

Indoor air quality is an influential factor in human health. To achieve a standard of comfort, it is necessary to have an interaction of variables, such as the optimization of relative humidity, temperature, and measurements of indoor air quality. Another important factor is the need for air renewal in the environment. Low rates of air exchange in indoor environments cause a considerable increase in chemical and biological pollutants in the air. Chemical products comprising volatile organic compounds, particulate matter, and others are released into the air from everyday products, various constructions, and processing tools. The largest is fresh construction materials. In general, it is common to spend more time working, living, or in leisure activities indoors. Nowadays, this topic is gaining more and more attention in debates and research, such as the concern to reduce its risks, as it is a matter of public health.

For these reasons, it is crucial to decide on air abatement technology to clean the air effectively and efficiently. In this master thesis, a prototype is analyzed to decompose the VOC concentration, where terpene is applied to the airflow to create an atmosphere with VOCs so that its decomposition can be investigated. This device is divided into stages: non-thermal plasma, UVC photolysis, bipolar ionization, electrostatic precipitator, and an ozone destructor. In this prototype, advanced oxidation processes are utilized to remove aerosol particles in the complex air cleaner device.

The study aims to investigate the efficiency of the complex air cleaner prototype by observing how aerosol particles as a by-product of the VOCs oxidation/decomposition process are generated at different air cleaning device stages.

The objectives are: An overview of scientific literature on VOCs as an indoor pollution source, as well as aerosol particles generation as a by-product of the VOCs oxidation/decomposition process and its removal technologies; To create a research plan and prepare a methodology for generated aerosol particle sampling in the complex air cleaner prototype; To evaluate the influence of individual complex air cleaner module parameters (bipolar ionization power and the number of UV lamps) on the generation of aerosol particles; To determine the dependence of the generated aerosol particle removal efficiency (efficiency of electrostatic precipitator) on the process parameters. Experiments utilized ELPI+ Dekati as an analytical instrument to measure real-time particle number concentration of the aerosol formation at each sampling point.

As a result of it, the particle size distribution and total suspended particles were plotted and analyzed. The initial concentrations had smaller diameters and higher concentrations, however, when observing the data at different sampling points (after the reaction chamber where the particles passed through UVC photolysis and bipolar ionizer), it had a slighter decrease in concentration, and

the influence of a number of the UVC lamps and bipolar ionizer did not appear to affect the relationship of increase in gas-to-particle conversion rate. At the last sampling measurement point, a significant decrease in concentration occurred leading to an increase in particle size. Overall, the complex air cleaner prototype had a removal efficiency of approximately 99,7%.

Santrauka

Patalpų oro kokybė daro didelę įtaką žmonių sveikatai. Komfortiškos sąlygos gali būti pasiektos esant tam tikrų kintamųjų sąveikai, pvz., optimaliai santykinei drėgmei, temperatūrai ir patalpų oro kokybei (mikroklimatui). Kitas svarbus veiksnys gerai patalpų oro kokybei – tinkamas oro apykaitos lygis. Žemas oro apykaitos lygis patalpose padidina cheminių ir biologinių teršalų kiekį ore. Patalpų aplinkos ore veikiant aktyviems ir pasyviems veiksniams į orą patenka įvairūs teršalai, tokie kaip lakieji organiniai junginiai, kietosios dalelės ir kt. Didelė organinių teršalų emisija atsiranda iš naujų statybinių medžiagų. Įprasta, kad daugiau laiko praleidžiama dirbant, gyvenant ar užsiimant laisvalaikio veiklomis uždarose patalpose. Šiais laikais ši tema sulaukia vis daugiau dėmesio diskusijose ir tyrimuose, rūpinamasi kaip sumažinti jos riziką, nes tai yra visuomenės sveikatos klausimas.

Dėl šių priežasčių labai svarbu apsvarstyti oro taršos mažinimo technologijas, kad oras būtų išvalytas efektyviai. Šiame magistro darbe analizuojamas eksperimentinis inovatyvaus kompleksinio oro valymo įrenginio prototipas, kuris skirtas LOJ teršalams skaidyti. Lakus organinis junginys – terpenas, buvo pasirinktas kaip teršalas, siekiant ištirti jo skilimo procesus. Kompleksinio oro valymo įrenginio prototipas skirstomas į kelis etapus: neterminę plazmą, UVC fotolizę, bipolinę jonizaciją, elektrostatinį nusodintuvą ir ozono destruktorių. Šiame prototipe naudojami pažangūs oksidacijos procesai, siekiant pašalinti aerozolio daleles sudėtingame oro valytuvo įrenginyje.

Tyrimo tikslas – ištirti eksperimentinio inovatyvaus kompleksinio oro valymo įrenginio prototipo efektyvumą, stebint, kaip aerozolio dalelės, kaip šalutinis LOJ oksidacijos/skilimo proceso produktas, susidaro skirtingose oro valymo įrenginio stadijose.

Tikslai: Apžvelgti mokslinę literatūrą apie LOJ, kaip patalpų taršos šaltinį, taip pat aerozolių dalelių susidarymą kaip LOJ oksidacijos/skilimo proceso šalutinį produktą ir jų šalinimo technologijas; Sudaryti tyrimo planą ir parengti generuojamų aerozolių dalelių mėginių ėmimo kompleksiniame oro valytuvo prototipe metodiką; Įvertinti atskirų kompleksinių oro valytuvo modulių parametrų (bipolinės jonizacijos galios ir UV lempų skaičiaus) įtaką aerozolio dalelių susidarymui; Nustatyti susidarančio aerozolio dalelių šalinimo efektyvumo (elektrostatinio nusodintuvo efektyvumo) priklausomybę nuo proceso parametrų.

ELPI+ Dekati buvo naudojamas kaip analitinis prietaisas, skirtas matuoti susidariusių aerozolio dalelių koncentraciją realiu laiku kiekviename mėginių ėmimo taške.

Šiame darbe buvo grafiškai atvaizduotas ir išanalizuotas dalelių pasiskirstymas pagal dydį ir bendras suspenduotų dalelių kiekis (skaitinė koncentracija). Pradinės koncentracijos buvo mažesnio skersmens ir tankesnės, tačiau, stebint duomenis skirtinguose mėginių ėmimo taškuose (po reakcijos kameros, kurioje dalelės praeidavo per UVC fotolizę ir bipolinį jonizatorių), jų koncentracija šiek tiek sumažėjo. UVC lempų skaičius ir bipolinis jonizatorius neturėjo įtakos dalelių konversijos iš dujinės fazės greičio padidėjimui. Paskutiniame mėginių ėmimo matavimo taške, po elektrostatinio nusodintuvo, žymiai sumažėjo dalelių koncentracija, todėl padidėjo dalelių dydis.

Kompleksinio oro valymo įrenginio prototipo aerozolio dalelių šalinimo efektyvumas siekė apie 99,7%.

Table of contents

List of figures

List of tables

List of abbreviations

Abbreviations:

ASHRAE – American Society of Heating, Refrigerating and Air-conditioning Engineers;

AOP – Advanced oxidation process;

AOT – Advanced oxidation technology;

CO – Carbon Monoxide;

DBD – Dielectric barrier discharge;

ESP – Electrostatic precipitator;

IAQ – Indoor air quality;

NAAQS – National Ambient Air Quality Standards;

NOx – Nitrogen oxides;

NTP – Non-thermal plasma;

ODC – Ozone decomposition catalyst;

O_3 – Ozone;

PM – Particulate matter;

PNC – Particle number concentration;

PSD – Particle size distribution;

Prof. – Professor;

SOA – Secondary organic aerosol;

SO_2 – Sulfur dioxide;

TSP – Total suspended particles;

US EPA – US Environmental Protection Agency;

VOCs – Volatile organic compounds;

WHO – World Health Organization.

Introduction

Many people are attentive of the environmental and health consequences of outdoor air pollution but may not realize that indoor air pollution can have severe consequences. Previously, the main focus was on the outdoors due to negative health effects and its demands. Scientists began examining complaints that occurred in the internal working environment around 1970, and according to the US EPA's study of human exposure to air pollutants, internal air levels of a number of pollutants could be two to five times higher than external levels [1].

Life has changed dramatically in recent decades, particularly in developed countries. People stay more time indoors due to rapid industrialization and urbanization, technological advancement, and occupational activities [2]. Nowadays, the environmental quality of air has a major effect on health and comfort, since it is believed that the majority of people devote approximately 90% of their own time indoors, whether at home, working, educational institutions, retail stores, or even transportation infrastructure. Indoor air quality has been observed to be a major concern because numerous diseases have frequently been a consequence of inner air contamination [1, 3].

Indoor air pollution ranges according to the characteristics of the building (base situation and type, the influence of mechanical ventilation, airtightness, envelope integrity), occupant behavior (interior smoking, cleaning product lines and use, air circulation routines), and analysis of environmental characteristics (climatic conditions and physiological context) [4], the rate these chemicals circulate from the outdoors into the indoors, involving the rate at which they are scavenged by various surfaces, captivated by internal chemical reactions, and eliminated by airflow/air cleaning, affects the concentration of chemicals [5].

These pollutants incorporate an extensive variety of organic and inorganic composition in the gaseous phase and in the particle phases. Most indoor air pollution is caused by the penetration of outdoor pollutants, and indoor pollutants sources comprise of food cooking, home appliance, heating, and mankind, those have rapid temporal change, construction materials emissions have gradual temporal variation, and it can be categorized by different diameter ranges (PM, VOCs, carbon dioxide, nitrogen oxides, etc) [6], inhalation per example VOCs could lead to sick building syndrome, headaches, fatigue, and many other diseases [7].

As a result, enhancing indoor air quality is developing into a more relevant matter. Several guides, regulations, and tools help create primary standards to establish limits related to public health protection for the primary pollutant, high priority providing information for indoor air quality applications, such as the ASHRAE standard, NAAQS, etc. [8]. As a basis, treatment and reduction of air pollutants using effective materials and methods are critical [7]. The use of integrated devices for the destruction of pollutants using oxidations (ozone), catalysts, and filters was identified as a feasible approach to improving IAQ, and air purification has turned into the most popular technique to enhance IAQ by removing VOC contaminants [9, 10].

This master's thesis aims to investigate the efficiency of the complex air cleaner prototype by observing how aerosol particles, as a by-product of the VOC oxidation/decomposition process, are generated at different stages of the air cleaning device.

The objectives of this master's thesis are the following:

1. Overview of scientific literature on VOCs as a source of indoor pollution, as well as aerosol particle generation as a by-product of the VOC oxidation/decomposition process and its removal technologies;
2. Create a research plan and prepare a methodology for aerosol particle sampling generated in the complex air cleaner prototype;
3. To evaluate the influence of the parameters of the individual complex air cleaner module (bipolar ionization power and number of UV lamps) on the generation of aerosol particles;
4. Determine the dependence of the generated aerosol particle removal efficiency (efficiency of the electrostatic precipitator) on the process parameters.

1. Literature review

1.1. Air pollution

Air pollution is a global concern that reduces the quality of ambient air and, as a result, people's lives indoors and outdoors. According to the WHO, it is classified as indoor/outdoor environmental contamination by any chemical, physical, or biological means that alters naturally occurring atmospheric features [11, 12]. As the world's population grows, air pollution will continue to be a problem, causing health and even mortality issues. The World Health Organization consider that more than 91 percent of people inhale inadequate air quality [12].

Nowadays, people consume more time indoors, and IAQ (indoor air quality) affects the individual health, well-being, and work rate. Larger air pollution hazards can contribute to poor human health, for example sickness, sick-building syndrome, and, in certain cases, cancer [13]. The sources of indoor pollutants (Table 1) exposed now differ from those of a few decades ago, because building components have been updated for polymers, new paint technologies, chemically treated materials, and others. The deterioration of interior quality can be associated to aspects of current construction methods and compositions, such as airtightness and an insufficient ventilation rate [14].

Table 1. Sources, health effects and guidelines of different pollutants [3, 17, 18]

Pollutant	Sources	Health effects	Guidelines
NO_2	Heating appliances, gas-fueled cooking	Respiratory damage, increase asthmatic reaction	0,15 mg/m^3 per 24h by WHO
O_3	Outdoor sources, air purifying, disinfecting machines, photocopying	Lung damage, throat irritation, coughing, asthma, diminish of respiratory functions, DNA damage	0,15-0,2 mg/m^3 per 1h by WHO 0,235 mg/m^3 per 1h by USEPA
SO_2	Outdoor air, fireplace, cooking stoves	Cardiovascular disease, asthma, impairment of respiratory function	0,35 mg/m^3 per 1h by WHO 0,365 mg/m^3 per 24h by USEPA
CO_x	Tobacco smoke, fireplaces, gasoline equipments, cooking stoves, outdoor air	Reduced brain function, fatigue, chest pain, headache, dizziness. High levels can cause loss of consciousness and death	CO: 30 mg/m^3 per 1h by WHO CO_2: 1800 mg/m^3 per 1h by WHO
Aerosols	Building components, incense burning, tobacco smoke, consumer products	Lung cancer, discomfort and irritation, cardiovascular diseases, allergies	0,15 mg/m^3 per 1h by USEPA
Radon	Soil gas, construction components, tap water, outdoor air	Lung cancer	100 Bq/m^3 per 1 year by WHO
VOCs	Paints, solvents, pesticides, adhesives, waxes, tobacco products, perfumes, plastics, dyes, lubricants, etc.	Headache, nausea, injury to kidney, central nervous system, eye/nose, some of them can cause cancer	Formaldehyde: 0,1 mg/m^3 per 30 min average by WHO
PM	Combustion activities (burning candles, stoves, chimneys, cigarette smoking), outdoor environment	Respiratory symptoms, lung function decrease, premature death, asthma	0,15 mg/m^3 per 1h by USEPA

Construction materials and human activities are the primary contributors to indoor pollution. Endogenous sources (long-term emissions from materials such as wood, paints, insulators, and sporadic sources, which are associated with activities such as hygiene and personal care); indoor reaction products (secondary sources, as secondary contamination production from the response in the gas phase being exposed to a chemical reaction on the surface of materials); and outdoor transfers (frequent outdoor sources are associated with anthropogenic pollution such as manufactories, fossil fuel combustions, and vehicle traffic entering indoors by natural and mechanical ventilation, as well as infiltration) [14, 15].

The principal air pollutants are dangerous gases, liquids, or solids because they possess higher-than-normal concentrations that decrease environmental quality [16]. They are classified into four types: inorganic, organic, radioactive, and biological. Many of them are detrimental to human health and indoor air quality. Volatile and semi-volatile organic compounds (VOCs), NOx, CO, PM, O_3, radon, microorganisms, and hazardous metals are the primary contaminants. The origins and effects of some contaminants are listed in Table 1 [3]. The technological options for the elimination of VOCs are of special interest in this work. As a result, some basic information about VOCs is also provided.

1.2. VOCs

Volatile organic compounds are a wider class of substances defined as any organic compound with a boiling point selection between $50 - 100\ ^oC$ to $240 - 260\ ^oC$ and a saturation vapor pressure of more than 102 kPa at room temperature [19]. These chemicals have an impact on air quality and include alkanes, alkenes, alcohols, carboxylic acids, aromatic hydrocarbons, and others. Table 2 shows the classification of VOCs based the chemical constitution.

Table 2. Classification conformable to chemical composition [20]

VOC group	Name	Structure
Aliphatic	Acetone; Formaldehyde	
Cyclic	Cyclohexane; Cyclohexanone	
Aromatic	Benzene; Toluene	
Polycyclic aromatic	Pyrene; Anthracene	
Nitrogen containing	Acetonitrile; Peroxy-acetyl-nitrate	
Halogen containing	Trichloroethylene; Tetrachloromethane	

Compounds can be naturally or anthropogenically emitted, with natural sources including oceans, volcanoes, and forests, and man-made sources including industries, solvents, and combustions [19, 21]. These chemicals are resistant to degradation and can be transmitted over long distances to the environment [22]. Fig. 1 shows the sources of outdoor VOCs, while Fig. 2 shows the sources of indoor VOCs.
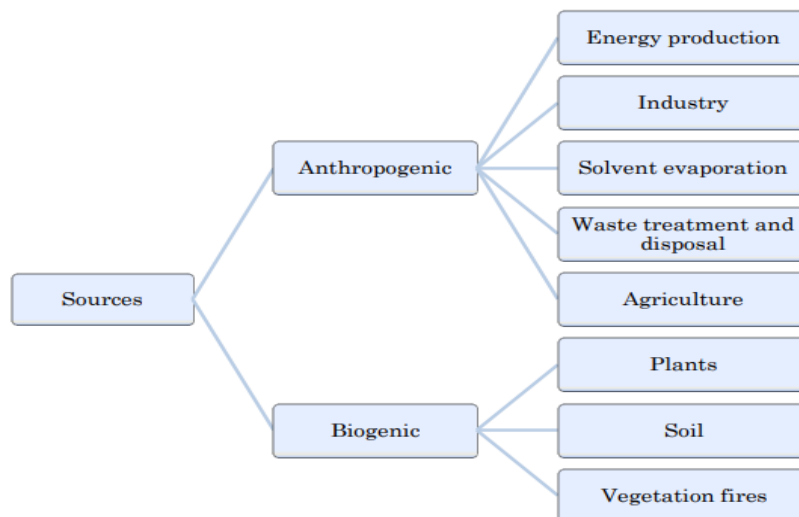
Fig. 1. Sources of VOCs [20]
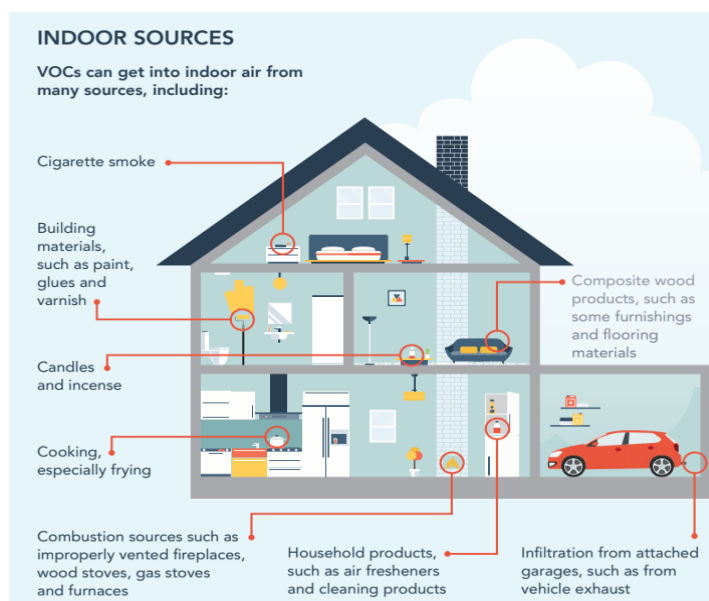
Fig. 2. Indoor sources of VOCs [23]

– VOCs classification

Under normal atmospheric pressure and temperature conditions, organic compounds evaporates; photochemical reactions in atmosphere also takes place, with exceptions from the EPA that contain imperceptible photochemical reactions; some VOCs can be more volatile than others, posing a greater risk to humans and the environment; and pollutants are distributed into: VVOCs (Very volatile organic compounds), VOCs (Volatile organic compounds), and SVOCs (Semi-volatile organic compounds) [22, 24]. Table 3 contains the classification of VOCs.

Table 3. Classification of VOCs [22, 24]

Abbreviation	Name	Information	Boiling point range °C	Examples
VVOCs	Very volatile organic compounds	Toxic at very low concentrations	<0 to 50-100	Propane, butane, methyl chloride
VOCs	Volatile organic compounds	It can be found in household products and be present in the environment	50-100 to 240-260	Formaldehyde, d-Limonene, Acetone, Toluene, ethanol
SVOCs	Semi-volatile organic compounds	It has higher molecular weight and boiling point; it is less likely to become vapor at room temperature	240-260 to 380-400	Pesticides, plasticizers, fire retardants

- **Effects**

In terms of environmental effects, global warming can be attributed to atmospheric gases known as greenhouse gases, which include H_2O, CO_2, CH_4, O_3, CFCs, and N_2O. Another result is the depletion of the ozone layer and the creation of photochemical smog, with ozone being the primary pollutant generated from the interaction of NOx and VOCs in the presence of UVB light [20].

The health influence of VOCs can assort from short-term and long-lasting depending on the concentration in the air, the dose, and the time of exposure. It has been shown that VOC concentration in indoor areas is up to two to five times higher than outside because, when in a heated indoor space, the majority of them evaporate, having concentration and composition greatly dependable on the activity undertaken. Exposure occurs by inhalation and ingestion, with skin contact being a minor route in this case. Air pollution contributes to food and water contamination, which is a key route of intake [25, 26].

Aromatic chemicals and carbonyls, such as benzene, toluene, and HCHO, are human carcinogens and contribute to the generation of smog in photochemical reactions. Short-term symptoms include headaches, dizziness, irritability, sick-building syndrome, and asthma, while long-term complications include leukemia, nasal tumors, and impaired pulmonary function [27]. Fig. 3 illustrates the effects of exposure to VOCs.

fatigue   nausea   dizziness   headaches   breathing problems   irritation of the eyes, nose and throat

Fig. 3. VOCs exposure effects [23]

1.3. Control methods

Approaches are used to minimize indoor pollution and improve indoor air quality. There are several ways that focus on eradication, substitution, or imprisonment. Another way would be to improve the ventilation system for the concentration dilution of interior pollutants by increasing the outdoor air volume; however, this is not the greatest solution because it may carry additional outdoor

pollutants, increasing the hazard. The final technique is linked to air purification technologies [28]. A description of air-cleaning technologies is provided below in Fig. 4.

Technology	Description	Contaminant
Media filtration	Porous media	Particles
Sorbents	Physio- or chemosorbents	Organic and inorganic gas-phase
UVC/UVGI	Ultraviolet (UV) lamp	Bioaerosols (airborne or on surfaces)
Photocatalytic oxidation (PCO)	UV lamp and photocatalyst	Organic and inorganic gas-phase (occasionally bioaerosols)
Electronic air cleaners (EACs)	Corona or pin ionizer, enhanced deposition in or out of device	Particles
Plasma	Electrical discharge	Organic gas-phase
Catalyst	Excludes PCO photocatalysts	Organic and inorganic gas-phase
Plants	Various botanical systems	Particulate and gas-phase
Ozone	UV or corona generation of ozone	Organic gas-phase (occasionally bioaerosols)

Fig. 4. Air cleaning techniques [29]

To improve IAQ, the following recommendations are made: reduce interior emissions, adequately ventilate and avoid outdoor pollution. When there is no way to reduce or manage pollution, air cleaning systems must be used [28]. Depending on the class of contaminants to be removed, various devices are used to reduce contaminants in buildings by physically removing air contaminants such as particulate matter, gases, and vapors or by participating in chemical reactions aimed at producing innocuous substances [30]. Fig. 5 illustrate different processes for pollutants and their efficiency are illustrated.

Process	Dust	Heavy Metals — Particulate	Heavy Metals — Gaseous	Acid Gases — HCl, HF, HBr, HI	Acid Gases — SOx	NOx	CO	CO2	Dioxin Furan	VOC	Odours
Cyclones	■										
Venturi Scrubbers	■■	■■	■■	■■					■		■■
Sleeve-Bag Filters	■■■	■■■							■		
ESP Filters	■■■	■■									
Dry Scrubbers	■■■	■■■	■	■■	■				■		
Wet Scrubbers	■■■	■■■	■■	■■■	■■■			■■■	■		■
Selective catalytic reduction (SCR)						■■			■■■		
Thermal Oxidation							■■■			■■■	■■
Catalytic Oxidation							■■■			■■■	■■
Chemical Absorption	■■	■■	■	■■■			■■	■■			■■■
Adsorption			■■■	■	■		■	■	■■■	■■■	■■■
Photo-Oxidation						■■■				■■	■■■
Condensation										■■	
Bio-Filtration										■■	■■■

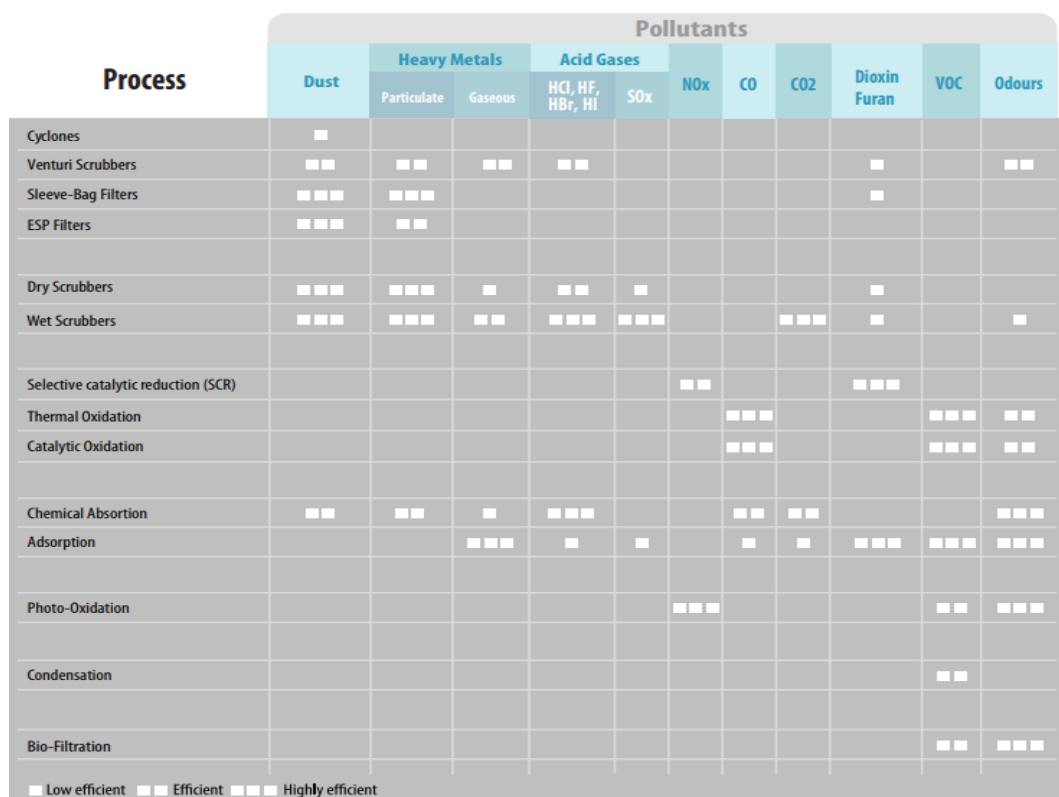□ Low efficient   □□ Efficient   □□□ Highly efficient

Fig. 5. Pollutants in different processes and its efficiency [31]

In relation to the VOCs removal method consisting of physical, chemical, and biological approaches by recovery or destruction, the scheme is shown in Fig. 6.
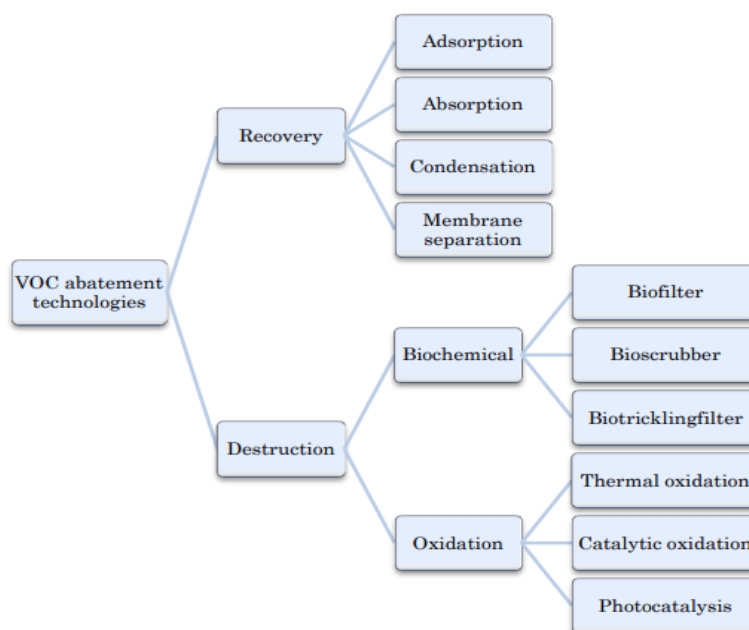
Fig. 6. Traditional technologies for VOC control [20]

The most prevalent procedures for removing VOCs from the air include sorption/decomposition by UV radiation, oxidation by plasma and catalyst, ozonation, and biological solutions [32, 33]. However, with the usage of these technologies at small concentrations, it is necessary to develop alternative technologies, such as nonthermal plasma for the decomposition of these contaminants because these devices are low cost, maintenance free-operation, and have good efficiency, cause less harmful by-products, including water, CO_2, and HCl gas, however, due to technological limitations, when there is a higher pollutant concentration, organic monomers molecules polymerize in the plasma environment, turning particles into secondary pollutants and creating a negative impact on the reactor [34].

1.3.1. Oxidation of VOCs

Considering the drawbacks of VOC removal methods such as catalytic oxidation (its efficiency-sensitive operation condition), and thermal oxidation as high energy utilization, the advanced oxidation process (AOP) highlights the fact that it is energy efficient and effective in removing VOCs, operates at ambient temperature and atmospheric pressure, and is suitable for multiple-component VOCs [33, 35].

Advanced oxidation technology (AOT) is a process that decomposes organic compounds (e.g., dissolved hydrocarbons, nitrogen, and sulfur oxides) through hydroxyl atoms (OH). Previously, the process was used for water treatment using OH radicals and hydrogen peroxide photolysis but has now been used for gas treatment as pollution control. In addition, hydroxyl radicals do not produce additional waste, hazardous chemicals, or corrosion of equipment [37].

The 4th state of matter (Plasma) is based on ions and electrons that occurs in a fully or partially ionized gas produced by electrical discharge variation; it can be characterized as a thermal plasma or a non-thermal plasma [36, 38].

Non-thermal plasma (NTP) is a sort of advanced oxidation (AO) in which VOCs are oxidized by powerful oxidative radicals, creating free radicals and oxidant species such as O_3, O, OH, and HO_2

19

before converting into CO_2 and water. This technique is utilized for indoor air cleaning [28, 33]. Corona, surface, and dielectric barrier discharges are the most prevalent for gaseous contaminants, with corona discharge and DBD being the most common [35].

The basic objective behind this process is by discharging a neutral gas to produce a quasi-neutral condition comprised of ions, radicals, UV photons, and electrons. While heavy ions continue cold owing to the transfer of energy caused by collisions with the surrounding gas, the electrons have their velocity increased by the magnetic field to raise the temperature [39], this causes the oxidation and ionization of the air molecule (O_2, N_2, H_2O) by induced voltage. It leads to the decomposition and conversion to CO_2 and water (OH, HO_2, O, N, H, as well as O_3, and H_2O_2). Yet, the drawbacks of this method include low mineralization efficiency, and undesired by-products such as O_3, NOx, and intermediate organic products (CO, hydrocarbons, deposits which can be more toxic than the VOCs) [35, 40].

1.3.2. NTP by-product formation

Unwanted products are produced as a result of the unexpected interaction of active particles and impurities. The causes are free radicals' high reactivity, fast chemical reactions compelling free radicals, and the appropriate clearness for acceptable conduction of energy and by-products. The principal by-products are created by plasma-catalyzed VOC removal systems. Organic and inorganic chemicals are frequent product components. Organic compounds are often intermediate compounds and solid formations of partial breakdown of target pollutants, whilst inorganic compounds frequently encompass ozone, nitric oxide, and COx [41].

The primary influences on the composition are plasma reactor kind, operational settings (applied voltage), and transported gas composition. Two major kinds: O_3 – It is the primary by-product of the NTP method for the VOCs eradication in the air [41].

The reaction with oxygen using high-energy electrons occurs during the removal of VOCs, and the process produce atomic oxygen, which is coupled with molecular oxygen to generate O_3. NOx (NO, NO_2, N_2O) is an undesirable by-product of processes involving excited nitrogen atoms and atomic oxygen [41].

The intermediate carbon radicals obtained from the initial removal of VOCs and produced in the plasma from the instability of radical leads to the removal of oxidative VOCs to COx, which can be produced in the NTP system by the collision of electrons with CO_2 [41].

The significance of electrons in the eradication of volatile organic compounds is frequently disregarded. Electrons produce O, N, OH, and excited nitrogen molecules which are more inclined towards the disintegration and oxidation of gaseous organic contaminants. The typical energy of electrons during a plasma reaction is crucial as it directly impacts the composed reactive group and the energy necessary for its formation [41].

1.4. Secondary pollutant of VOCs

Volatile organic compounds serve as initial contaminants that lead to secondary particulate matter, commonly referred to as aerosols, due to their high reactivity and oxidation products formed when created through nucleation, and condensation, the reactive uptake of oxidation products is caused by

the gas-to-particle conversion of low-volatile organic gases into particles, which undergo chemical and physical processes that transform composition and physical properties, such as terpenes, oxidation is done primarily through adding mechanisms, and therefore, the oxidation of these types of compounds is more likely to produce low-volatile products [42-47].

The Environmental Protection Agency defines aerosols as a combination of solid particles and liquid droplets present in the atmosphere, while certain types of aerosols such as dust, smoke, and dirt, are visible to the naked eye, others require the usage of an electron microscope for its detection [42-47].

Particulate matter is categorized into primary and secondary types, based on mechanism and compounds participating in its development. In unison, particulate pollution is commonly known as total suspended particulates (TSP). Primary PM is released in particle form at the source of emissions, like the chimney of an electricity-generating facility, while secondary PM generation is the outcome of chemical and physical reactions that contain many precursor gases [48, 49].

The impact of PM on both the environment and well-being is largely driven by the size of the particles involved, as the composition, origin, and size of suspended particles can vary greatly. On the basis of these particles are arranged by their aerodynamic diameter, with coarse and fine particles being the most common. PM_{10} and $PM_{2.5}$ invoke particles with diameters smaller than 10 and 2,5 micrometers, respectively, while ultrafine particles are those less than 0,1 micrometers in size [50, 51]. Fig. 7 illustrates the PM comparison in size.
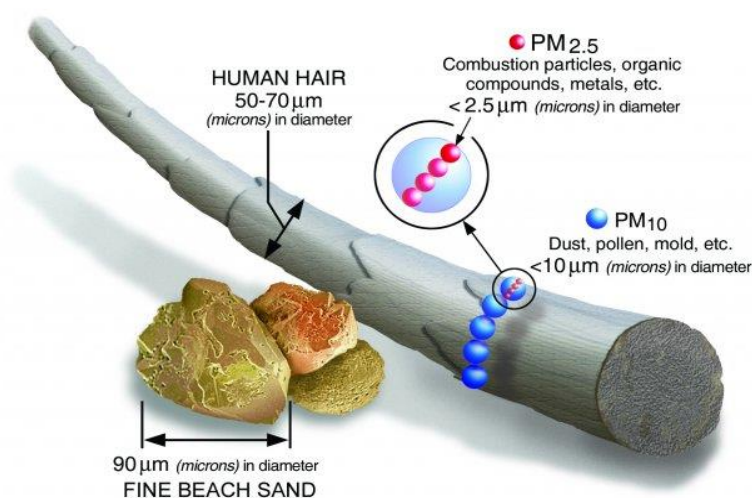
Fig. 7. Particulate matter particles comparison in size [43]

The presence of small droplets in PM can lead to respiratory and other health problems if inhaled. PM_{10} can penetrate the lungs and bloodstream, while $PM_{2.5}$ particles show aggravated risks. Airborne particles at high levels can negatively impact air quality and cause short-time irritation, immune responses, and breathing difficulties, while longer-time exposure results in premature death and cancer. $PM_{2.5}$ is linked to respiratory-related hospital admissions, asthma exacerbation, and early mortality [16, 48]. Table 4 illustrates the particle penetration in the human body.

Table 4. Particle size penetrability [16]

Particle size	Penetration degree in human respiratory system
>11 μm	Entry into nasal cavity and upper respiratory system
7 - 11 μm	Entry into nasal cavity
4,7 - 7 μm	Entry into the larynx
3,3 – 4,7 μm	Entry into the tracheobronchial region
2,1 – 3,3 μm	Transit through the secondary bronchioles
1,1 – 2,1 μm	Bronchial area terminal passage
0,65 – 1,1 μm	Bronchioles penetration
0,43 – 0,65 μm	Alveolar penetration

1.5. Multi-stage air cleaner technology prototype of advanced oxidation system

This prototype is used in an advanced oxidation gas-to-particle conversion system to reduce volatile organic compounds in specialized applications. Aerosol particles arise from non-thermal plasma, and through the bonding of partially oxidized compounds, they evolve into larger molecular structures in their solid-state form; in the gas-to-particle conversion, this occurs unintentionally while decomposing VOCs, laying the groundwork for VOCs elimination in a multi-stage air cleaner [32, 33]. The data are collected using ELPI+ Dekati. Fig. 8 Its process stages.
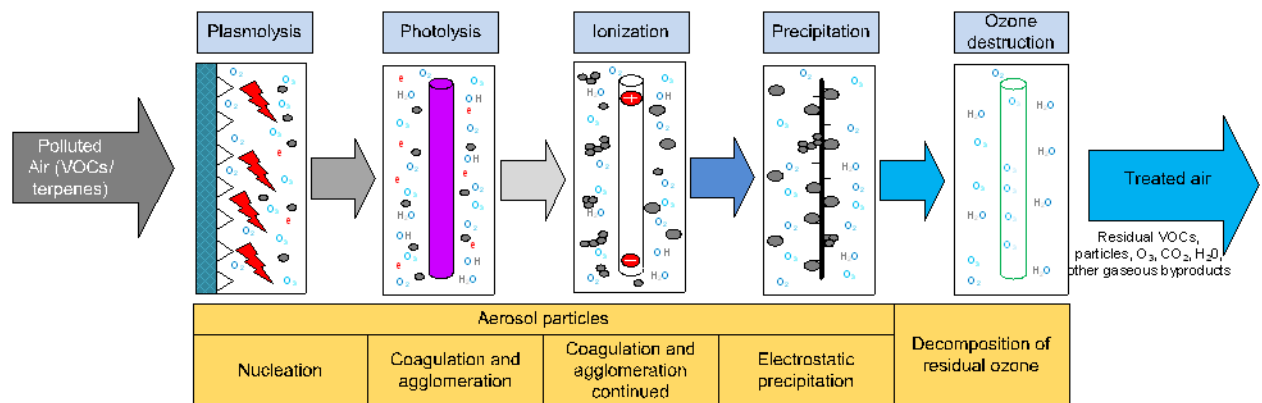
Fig. 8. Prototype process stages

The multi-stage process entails a series of steps, beginning with:
- The activation of particle formation through the use of **non-thermal plasma**;
- Subsequently, **UV radiation** is employed to stimulate growth in the diameter of the particle;
- Followed by **bipolar ionization** for the agglomeration of particles;
- The final stages include the utilization of an **electrostatic precipitator** to eliminate particles from the airstream;
- And an **O₃ destructing catalyst** for the decomposition of residual O_3 and reactive radicals.

1.5.1. Plasmolysis

First, the air polluted by plasma decomposition is used in a study to input oxidized species. Plasmolysis utilizes two methods: a) if when the NTP is equipped with an ozone generator via an external unit-based DBD reactor that produces ozone, ozone is guided to a non-thermal plasma as a powerful oxidizing agent (O_3). The Ozonator converts oxygen from room temperature and dry air, concentrated oxygen into ozone by applying energy to the conversion of oxygen molecules (O_2). When the oxygen molecule is recombined, the generator charges the air flowing through it [52]. When organic compounds get into connection with ozone, it eliminates oxidative pollution and neutralizes organic odors containing carbon as the basic element; b) In-situ corona discharge from the NTP reactor, it produces oxidized species in parallel with plasmolysis of VOCs compounds in contaminated airflow [53].

By utilizing electrical discharges (corona discharge or DBD), the manipulation of various parameters including the discharge's operating voltage, the variable plasma density by power, which controls the number of ionizations; the pressure of the gas and the type of gas, can allow for control over the energy of charged particles in the plasma and the frequency of electron collisions. The electric field is changed by modifying the electrodes shape [53].

The DBD is utilized in the Ozonator, chemical vapor deposition, and decomposition of CO_2. It normally has 2 electrodes arranged asymmetrically on simultaneous walls of a dielectric barrier component, its purpose is to restrict the electric current and impede spark formation, corrosion and electroetching are caused by electrodes directly contact the plasma and the discharge gas differing from others in plasma discharges [54].

1.5.2. UV photolysis

The creation of aerosol particles is caused by photolysis by UV-C radiation which produces OH radicals from the produced ozone and vapor of H_2O. The molar extinction coefficient of a molecule influences its breakdown by UV photolysis; A compound with a high molar extinction coefficient can absorb more UV energy and thus be utilized for decomposition [55].

The introduction of UV wavelengths into the atmosphere can trigger a reaction with volatile organic compounds, resulting in the formation of aerosol particles. These particles undergo a transformation process through photo-oxidation, evolving into a less volatile partial oxidation products that ultimately coagulate and create new aerosols or larger SOA [56].

In the wavelength range of 100 to 1000 nm, UV radiation has the ability to eliminate air contaminants through a process known as photochemical dissociation. This procedure entails the absorption of photons by molecules, which excites the electrons and causes them to move from a low to a highly excited state. This destabilizes the photons and results in various reactions, including the discharge of light/heat and the dividing bonds chemically. Additionally, UV light of shorter wavelengths is particularly effective in removing air contaminants due to its high energy levels [57].

The efficiency of the UV photo-degradation process is shaped by a number of variables, among which the intensity of UV light, the duration of gas retention, the concentration of volatile organic compounds (VOCs), and the relative gas humidity. When UV light photons break down VOCs, this

process is called photolysis/photodecomposition. This method is one of two mechanisms for VOCs photo-degradation initiated by UV irradiation. The alternative route is photo-oxidation, in this process, O_2 and volatile organic compounds molecules are activated by UV light and undergo an oxidation reaction, producing active oxidants. Due to energy constraints of UV irradiation, not all VOC molecules are converted to CO_2. As a result, some intermediate organics will be produced during photo-degradation [45].

The utilization of oxygen from early hydrocarbons molecules to oxidize the intermediate led to the creation of high molecular weight particles and their subsequent exposure to UV light, as evidenced by carbon dioxide and intermediate data. Various types of studies have been published on the conversion of volatile organic compounds into SOAs in both the atmosphere and smog chambers, with particular attention given to the presence of NOx and sunlight. UV reactors need to be combined with another processing unit to reduce ozone and PM emissions [58].

1.5.3. Bipolar ionizer

In this stage, BPI technology, employs an artificial energy source to generate simultaneously cations and anions. The generation of these ions is achieved by altering the voltage to the electrodes, which produces an electric field. As contaminants flow rushes to this electric field, certain molecules and atoms within the airflow may acquire or give up electrons and ionize. The different types of bipolar ionizers, including corona discharge, DBD, are created through various electrical configurations [59]. Fig. 9 shows particle formation in the ionizer.
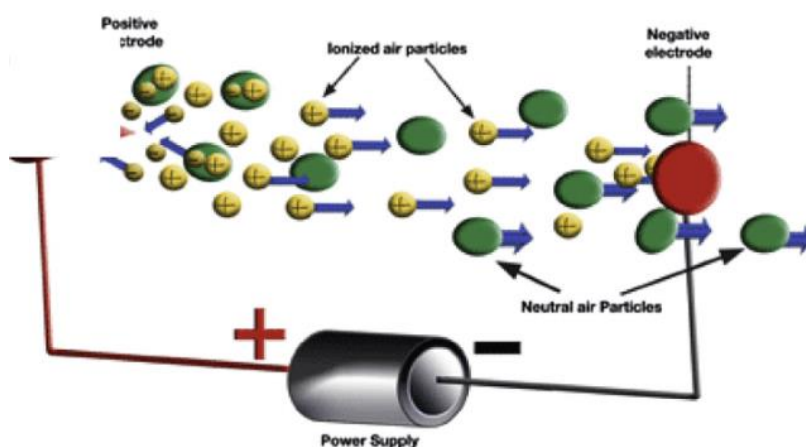
Fig. 9. Schematic anthropogenic pathways for ion particle formation [60]

Bipolar ionization has been shown to be effective in eliminating particles via a process known as agglomeration. Particles are attracted to ions and can draw more particles with opposing polarities to build bigger particles. These particles ultimately grow into sufficiently big to either settle on the ground, get collected by a filter, or adhere to further surfaces. The process of inactivating microorganisms and decreasing VOCs is more complicated [48].

Ionization energy, also known as ionization potential, is the quantity of energy needed to take one electron out of an atom or molecule. The ionization energy varies depending on the specific atom or molecule. The air composition and energy availability affect the kinds of ions of the BPI technology generated. When high levels of energy are present, a range of reactive oxygen molecules are

formed. These chemicals can then be capable of eliminating the atoms of H from the chains of carbon through a series of chemical reactions [46].

As a consequence, carbon chains in VOCs degrade, and VOCs can be degraded to CO_2 and H_2O. Ozone is also created at high energy levels during this process [59], as well as other likely dangerous by-products except certain safeguards are captured in product structure and upkeep [61].

VOCs neutralizers: OH molecules bind to hydrogen from such VOCs, disrupting its structural links. As a result, VOCs are converted to inert chemicals like O_2, N_2, CO_2, and water vapor. Several studies have shown that various VOCs have variable clearance rates, and that partial oxidation can occur, leading to equally toxic derivatives such as aldehydes [49].

When removing the particles, the bipolar ions adapt to the particles and begin to charge some negatively and others positively. When the particle cluster reaches sufficient mass, these oppositely charged particles are attracted from the air, coalesced, settled, and trapped in the filter. Nonetheless, studies have shown that many parameters, such as the type of wall surface of the treated space, particle concentration, particle size, and size of the treated space, can all affect the effectiveness of particle removal from the ionizer indicated by [62].

A study that particle in particulates drops resulting from agglomeration and conglomeration in particles in the air (by the agglomeration of airborne particulates, one can effectively reduce their concentration and facilitate their filtration or settlement) and VOCs oxidizes numerous airborne organic molecules to CO_2 and H_2O demonstrated the effectiveness of the BPI device [63].

Yet, a restricted quantity of other investigations have highlighted the ionization ability in the generation of different products, such as NOx and volatile organic compounds oxidation intermediates, despite the fact that there is minimal peer-reviewed literature on by-product generation [64]. The bipolar ionizer's reaction chamber has been used to slow down gas-phase chemical processes and enable the coagulation and agglomeration of aerosol particles, which increases aerosol particle size [32].

1.5.4. Electrostatic precipitator

In this phase, the aerosol particles produced were gathered by a needle plate electrostatic precipitator running at an elevated negative voltage. This technology is applied in particulate control devices, the utilization of the electric field in gas stream separates the wilfully charged particles by directing them to the field, causing them to move towards a capture plate with the opposite charge [65]. The efficiency is affected by the number of fields, residence period, and upstream particle elimination equipment [66], and the units treat huge gas volumes while achieving high collection efficiency by employing plate-collecting electrodes [67].

The high-voltage dc corona technique is widely used and highly dependable for particle charging. Within this apparatus, an energetic electrode of high voltage, akin to a slender wire, interfaces with a dormant ground electrode, perhaps in the form of a plate or pipe. The corona that surrounds the discharge electrode beckons forth ions of a positive or negative nature towards the gathering electrode. As a result, all particles that traverse this apparatus become electrified. These electrified particles are subsequently enticed towards the gathering electrode through the force of electrostatic attraction [68]. The fundamental operations of an electrostatic precipitator can be viewed in Fig. 10.
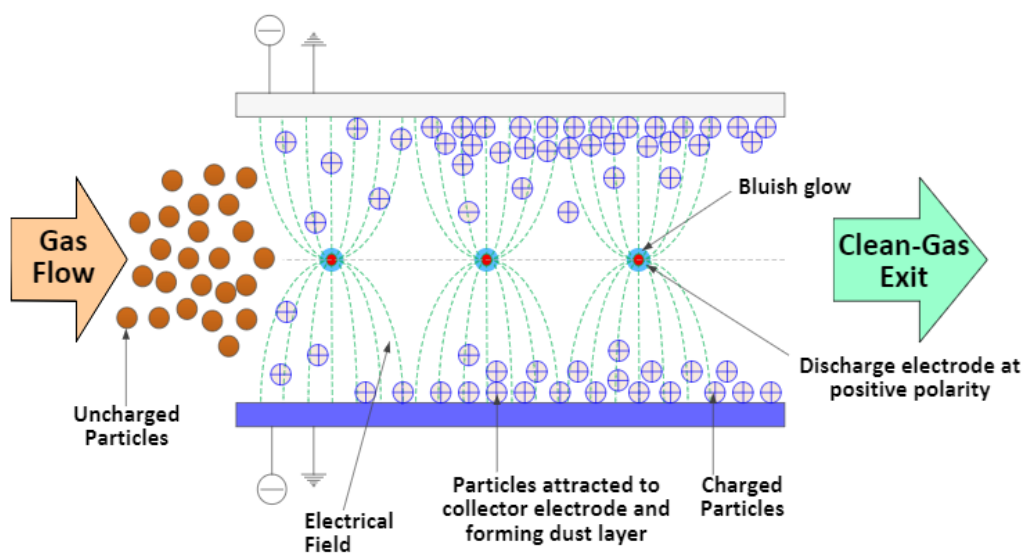
Fig. 10. Scheme of electrostatic precipitator [65]

ESPs are known to create a small quantity of ozone in the air stream; however, ozone production has been found to decrease using alternating voltage, and the electrostatic filtering efficiency of particles can range from 82 to 94 percent [69].

1.5.5. Ozone decomposition catalyst

The final stage of the system includes an ozone decomposition catalyst, which is a ceramic MnO_2^- embedded catalyst that acts as an O_3 destroyer. As per a study conducted, the surface of a MnO_2-based catalyst facilitates the generation of O atoms, O_2, and OH radicals from O_3. Essentially, the dissociative adsorption of ozone on the surface of the catalyst outcome in the formation of an O_2 and an atomic oxygen species. The atomic species then combines with other O_3 to produce peroxide and gas-phase oxygen molecule [57].

The most frequent reaction intermediate, which is the adsorbed peroxide, undergoes breakdown to produce gaseous O_2. This process elucidates the reason behind the metal oxide transition, which has many oxidation conditions that are readily accessible and serve as a potent catalyst for the decomposition of O_3. The method is composed of redox stages, namely, the adsorption of ozone on the catalyst and the removal of adsorbed intermediates. These stages occur at equal rates in a steady state; hence, the speed of the catalyst's oxidation and reduction determines the pace of the breakdown reaction [70].

Through the process of ozone catalytic oxidation, radicals are able to react with VOCs on the surface of the ODC. This reaction results in the decomposition and mineralization of the volatile organic compounds into CO and CO_2, effectively eliminating a variety of gaseous phase contaminants. However, it is important to note that excessive amounts of O_3 can be harmful to the health, and therefore, the elimination of O_3 must be proportional to the concentration of the ODC to maintain safe levels [71].

The majority of research on gas-phase O_3 decomposition focus on catalytic methods for the remove of O_3 from the environment. The noble metals are catalysts' active elements, but the high cost of it has stimulate the utilization of transition metals such as cobber, nickel, manganese, silver, etc. TiO_2,

SiO$_2$, zeolites, and activated carbon are employed as catalytic materials. Among the oxides employed in ozone breakdown, supported manganese oxides have been characterized as active oxides. Manganese oxides are often used to catalyze a variety of chemical processes, including nitric oxide reduction, CO, NH$_3$, methanol, and ethanol oxidation [72].

1.6. ELPI+

Within the realm of particle sizes, two similar approaches are often used: either the mobility dimension or the aerodynamic diameter. These concepts take into account the variation in size, mass, and morphology, the density of the particles acting as a connecting factor between them. Additionally, the particle's dynamic shape factor is a closely related quantity that describes how the shape of a particle affects its effective density. The airborne PSD is a crucial characteristic in evaluating work-related exposure and air quality. To predict the motion of particle in various contexts, such as in the atmosphere or in measurement devices, it is necessary to consider the effective density in conjunction with one of the equivalent diameters [73, 74].

Within the realm of modern workspaces and environmental air quality assessment, a plethora of tools (including the aerodynamic particle sizer, analyzing mobility particle sizer, and fast mobility particle sizer) are executed to gauge the PSD of airborne particles. Aerosol size distribution may now be measured online virtually continuously, thanks to the latest improvements in aerosol measurement [73, 74].

To provide real-time particle diagnosis, the ELPI+ is an electrical low-pressure impactor incorporating electrical sensing of ionized particles with a 14-stage of cascade impactor. For instance, air quality measurements, combustion aerosols, and engine exhaust gases are commonly carried out using this device. Because the mass of the collected particles on each substrate must be appropriately elevated to be detected by a sensitive microbalance, the sampling duration is highly correlated with the sampled particle mass concentration [75–77].

The ELPI+ consists of a triumvirate of essential elements - a cascade impactor, a unipolar diode charger, and a multichannel electrometer. The classification of particle sizes is accomplished through the use of the cascade impactor, which separates larger particles in the initial stage. The remaining 13 stages are linked to a multichannel electrometer, which measures the charge produced by the particles collected from each stage, using electrical insulators to keep them separate [75–77].

By monitoring the electric current from each stage, it is possible to identify the unipolarity-charged particles that settle on the stages. The filter is the last step, which collects sufficiently tiny particles to be deposited from the earlier steps through the cascade impactor. The impactor stage and the filter step are both linked to the electrometer. The number concentrations are then calculated from the current measurement signals using the charger's response function. The aerodynamic particle sizes dictate how the particles are gathered in various impactor stages. Correspondent to the response function, the observed current is correlated with the number concentration at various particle sizes [75–78].

Several variables, e.g., flow rates, particles entering the charger, and charging efficiency, shall be considered in the response function. A flush pump, a high-voltage power source for the charger, and related control electronics are all included in the instrument. The flush pump shall be utilized for the reset the electrometers by pushing clean air through the instrument [78].

When the flush mode is switched on, a pump built into the ELPI+ delivers filtered, particle-free air into the charging area. This allows for the electrometer zero levels to be checked and adjusted. Once the diffusion charger is turned off, the bipolar electrometers enable particle charge analyses. An in-built computer controls how the instrument operates [75].

1.7. The findings of the literature review

It was established that not only outdoor pollution but also indoor air pollution can have sequela for the environment and human health. Contaminants come from the outside and also into sources of indoor environment, VOCs, and also other pollutants, their principal exposure pathway is by inhalation leading to many diseases.

Several guides, regulations, and tools were created to set limits related to public health protection and indoor air quality applications. According to the WHO, air pollution is classified as any contaminant by chemical, physical, or biological means that alters atmospheric characteristics. Indoor pollution's primary contributors are construction materials and human activities.

Pollutants can be classified as organic, inorganic, radioactive, and biological. The main indoor air pollutants are NOx, CO, PM, O_3, VOCs, microorganisms, radon, and hazardous metals; different pollutants come from different sources and lead to health and environmental effects, guidelines were created to limit their concentration in the air.

VOCs are any organic compound with a boiling point from 50-100 ºC to 240-260 ºC and saturation vapor pressure of more than 102 KPa at room temperature. They include alkenes, alkanes, carboxylic acids, and others. Emitted by industries, solvents, and combustion sources either naturally or by man. Particulate matter known as aerosols can be caused by VOC decomposition in determined types of processes leading to a secondary organic pollutant.

VOCs consist of three classifications such as volatile organic compounds (VOCs), semi-volatile organic compounds (SVOCs), and very volatile organic compounds (VVOCs), being differentiated by their boiling point. VOCs' health impacts can dispose from short-term to long-term depending on their concentration in air, dosage, and time of exposure. It can lead to fatigue, nausea, breathing problems, and irritation of the eyes. Particulate matter is divided into fine and coarse particles, depending on the aerodynamic diameter classified as $PM_{2.5}$ and PM_{10}.

Control methods are approached by the use of eradication, substitution, or imprisonment, as well as air purification technologies. Depending on the class of contaminants, different devices must be applied to reduce contaminants in buildings.

The advanced oxidation process (AOP) is an effective procedure to remove VOCs at room temperature and atmospheric pressure by decomposing organic compounds through the OH radical. Non-thermal plasma is one of the examples of advanced oxidation by the creation of free radicals and oxidant species into the conversion of CO_2 and water, corona discharge and DBD are the most used. This method creates a quasi-neutral environment by discharging a neutral gas. Unwanted by-products such as NOx, COx, and SOA are formed by the interaction of active particles and impurities.

A prototype of a multistage air cleaner technology is developed to convert gas to particles by reducing VOCs in indoor applications. Multistage methods include plasmolysis, photolysis, ionization, precipitation, and ozone destruction. Each of the stages has its main principle. In non-thermal plasma, it occurs the initiation of particle formation, while UV radiation in photolysis to the growth of particle diameter, in bipolar ionization its agglomeration and the eradication of particles from the airstream is done by an electrostatic precipitator. Ozone destruction is used in the decomposition of residual ozone and reactive radicals remaining in the stream.

2. Research methodology

2.1. Research design

This chapter covers the overall approach of the research in detail that was employed in the subsequent result chapters to test the hypothesis of this work. Additional information on the experiment design is presented in the appropriate sub-chapter. The research design was carried out according to the objective of the study presented in Fig. 11.
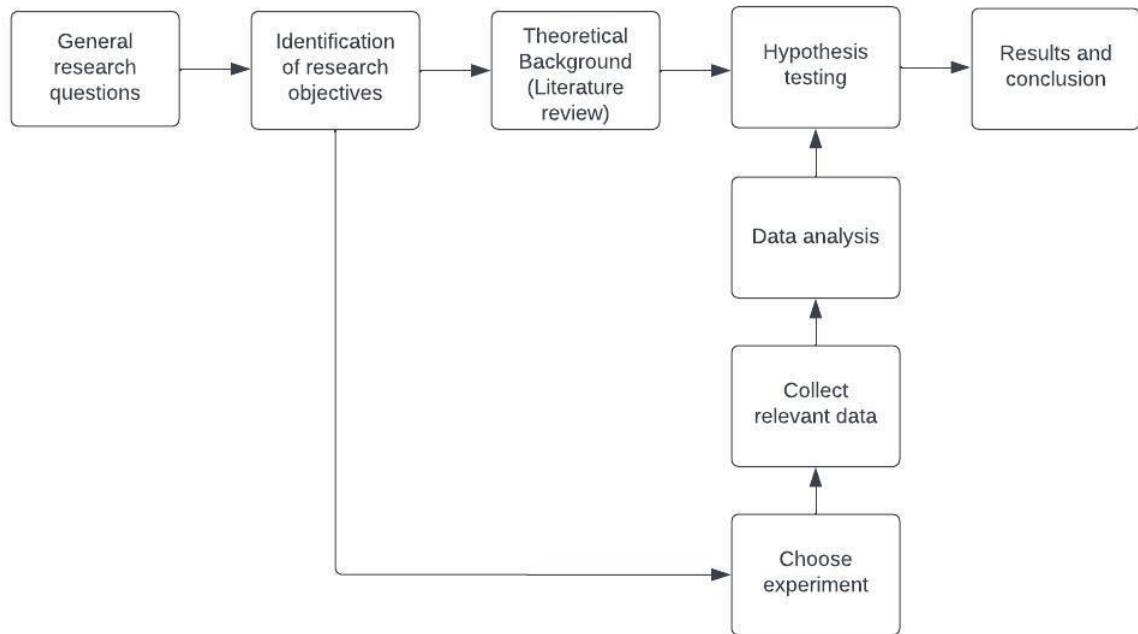
Fig. 11. Presentation of research design

This research tests the hypothesis that an increase in the bipolar power of the complex air cleaner prototype positively affects the growth of the gas-to-particle conversion rate, which results are expected to reject or support it. Nevertheless, an investigation of the aerosol particle growth mechanism and an overview of the generation of VOC oxidation/decomposition process and its removal techniques as well as evaluating the influence of individual complex air cleaner module parameters on generation of aerosol particles and determining the dependence of generated aerosol particle removal efficiency on the process parameters are going to be discussed.

2.2. Experimental set-up of the multi-stage complex air cleaner technology prototype

The complex air cleaner device is composed of a multistage prototype constructed in the Department of Environmental Engineering at Kaunas University of Technology. It consists of 5 stages, including plasmolysis (non-thermal plasma), photolysis (UV radiation), ionization (Bipolar ionization), precipitation (Electrostatic precipitator), and ozone destruction (Ozone decomposition catalyst). Fig. 12 below represents the prototype design.

Fig. 12. Prototype design set-up; S1, S2, and S3 are sampling points

The non-thermal plasma power and the electrostatic precipitator were set to be both constant at 15kV. Laboratory air and an air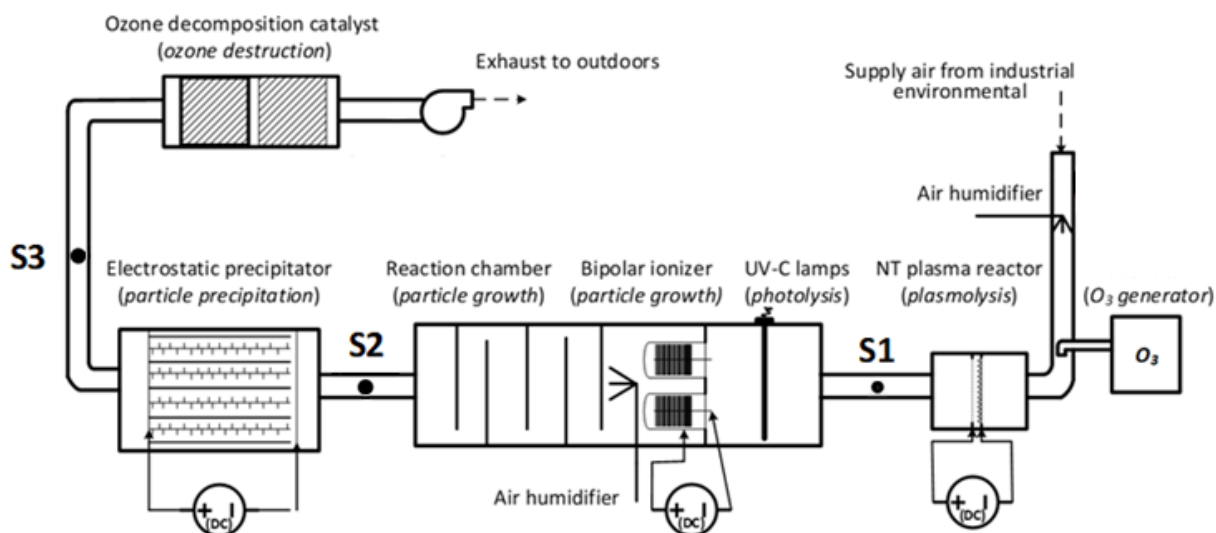 pump were used for constant air supply into the system and a digital anemometer was used to measure the linear velocity of airflow, the corresponding air flow rate was chosen at 25 m^3/h.

Volatile organic compounds (VOCs) were supplied into the device at the beginning of the reactor through the assistance of a syringe pump (Fig. 13), in it, terpene was pushed into the prototype to deliver a precise concentration of compound to the air chamber, the tube through which terpene flowed was wrapped with nichrome wire and heated to make terpene vaporize more intensively.

Fig. 13. Syringe pump [79]

As the terpene was heated and converted to vapor, it entered the system and was carried by air supplied by a pump through the device reactor. The study utilized a sealed air chamber made of aluminum, with inlet and outlet pipes connected to the ELPI+ and the prototype's air pipe, ensuring a consistent pollutant composition throughout the system. During operation in the NTP reactor, an electric field created a discharge, resulting in the formation of ozone, active radicals, decomposition of the terpene, and unwanted aerosol formation.

To evaluate the influence of the stages of the prototype device, two parameters were modified while conducting this experiment. First, the UVC lamps were changed from five lamps to zero lamps and the bipolar ionizer was changed from 10 to 14kV, respectively. It was set constant the flow rate (25 m^3/h), temperature (20 °C), NTP power (15 kV), electrostatic precipitator (-15 kV), the

31

concentration of VOC (5 mg/m^3), and relative humidity (50%). At each experiment run, one lamp was turned off and one voltage was chosen in the bipolar ionizer, starting the run with five working lamps. At each sampling point (S1, S2, and S3) aerosol particle measurements were taken. Table 5 provides the conditions for the experiment, and Fig. 14 shows the placement of the light bulb in the device.

Table 5. Experiment conditions under which measurements were conducted

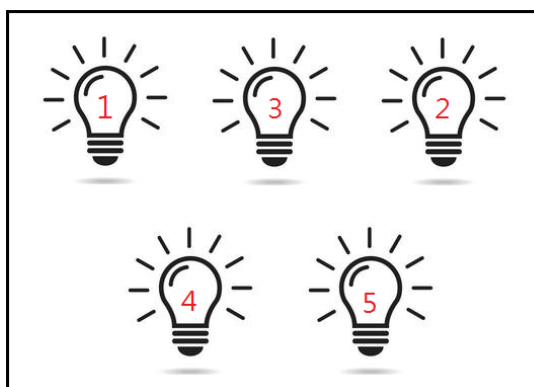| No. of experiment	Bipolar ionization, kV	UVC lamps, unit	Flow rate, m^3/h
N1	10	5	25
N2	11	5	25
N3	12	5	25
N4	13	5	25
N5	14	5	25
N6	10	4	25
N7	11	4	25
N8	12	4	25
N9	13	4	25
N10	14	4	25
N11	10	3	25
N12	11	3	25
N13	12	3	25
N14	13	3	25
N15	14	3	25
N16	10	2	25
N17	11	2	25
N18	12	2	25
N19	13	2	25
N20	14	2	25
N21	10	1	25
N22	11	1	25
N23	12	1	25
N24	13	1	25
N25	14	1	25
N26	10	0	25
N27	11	0	25
N28	12	0	25
N29	13	0	25
N30	14	0	25

Fig. 14. Representation of UVC light bulb placement setting

2.3. Analytical method

2.3.1. ELPI+ (Electrical Low-Pressure Impactor)

To determine the distribution of the size and concentration of aerosol particles, samples were collected in real-time utilizing the electrical low-pressure impactor (ELPI+, Dekati, Finland) (Fig. 15), this device segregates aerosol particles into 14 fractions (from 0,006 to 10,0 μm) corresponding to aerodynamic diameter by charging the particles in the corona discharge zone and leading to the multistage cascade impactor. Real-time aerosol concentrations are recorded at intervals of one-tenth of a second (10 Hz) and aerosol samples are collected on a 25mm diameter aluminum foil base coated with Apiezon L oil. The operating system and measurement data must be recorded on a PC. Before using the device in the experiment, ELPI+ was calibrated and cleaned [80–82].

Fig. 15. ELPI+ Dekati

To carry out the experiment, sampling points were chosen. The points where the measurement occurred were located: after non-thermal plasma (S1); after the reaction chamber (S2); and after the electrostatic precipitator (S3).

2.4. Data analysis and quality assurance

Data collected during the experiment were used for statistical analysis. The data obtained were processed and managed using Excel 2023 (Microsoft Inc., USA) and SPSS, based on descriptive statistics to summarize and visualize the concentration and distribution of aerosol particles. The

following main indicators of descriptive statistics were calculated: mean, median, standard deviation, minimum value, maximum value, 5th and 95th percentile. The median and mean were elected as central tendency measurements, data variability measurements were utilized by the standard deviation, minimum, and maximum values, and the 5th and 95th percentiles were measured to interpret the performance data [83].

The Mann-Whitney U test was utilized for the determination of the possibility of a statistically significant difference between the particle concentrations at the S2 sampling point using 10 kV and 14 kV. Particles under different conditions of experiments were compared with each other. If $p<0,05$, then it was concluded that the difference between the concentration of aerosol particles measurement was statistically significant.

In order to conduct a thorough statistical analysis, the data sample utilized was specifically chosen from the sampling points during the introduction of ELPI+ into the system. To prevent any aerosol losses, a sampling hose was designed to be as short as possible. It was imperative to stabilize the data for a brief period of 1,5 minutes after the measurement device was introduced. All diameters considered in this study were aerodynamic cut diameters with D50 values. Data collection was carried out for a duration of 2 minutes in S1 and 1 minute each in the S2 and S3 points.

The ELPI+ Dekati was utilized to measure the particle size distribution (PSD), the temporal fluctuations of particle number concentration (PNC) and PSD was established on the basis of particle units per cubic centimeter ($\#/cm^3$). PSD was derived from the distribution function of the number density (concentration) that reflects the concentration of particles normalized to their size area, defined between Dp and dDp. This is mathematically expressed as $Dp=dN/dlogDp$ ($\#/cm^3$) [80, 84].

The fluctuation of Particle Number Concentration (PNC) is a result of various factors such as ventilation, gravitational settling, adsorption in walls, diffusion, electrostatic forces, and thermophoresis [80].

The acquisition, preparation, and examination of samples were conducted with the utmost adherence to laboratory protocols. ELPI+ was cleaned in the laboratory before the start of the experiment.

3. Results and discussion

The results are presented as follows: the first subsection of results in descriptive statistics for the experimental data. Further subsections are the particle size distribution, total suspended aerosol particles, t-tests, Mann-Whitney U test, and aerosol particles removal efficiency of the prototype.

3.1. Descriptive statistics

Descriptive statistics were performed for the three sampling points (S1, S2, and S3), the modified parameters were the UVC lamps (from 5 lamps to zero lamps) and the bipolar ionizer power (from 10 kV to 14 kV). During one set of experiment containing 15 runs occurred that the same quantity of UVC lamps were applied from 10 kV to 14 kV, with different bipolar ionizer power parameters. The experiment had a total of 90 runs (30 runs for each sampling point).

For better understanding and visualization, Tables 6, 7, and 8, performed on descriptive statistics, were distributed according to the sampling point locations on the device.

Table 6. Descriptive statistics of indoor air concentration in the sampling point S1

S1, (25 m³/h)		Mean	Standard Deviation	Median	Minimum	5th percentile	95th percentile	Maximum
PNC, #/cm³	10 kV – 0 lamp	4,67E+06	2,44E+05	4,69E+06	4,08E+06	4,27E+06	5,07E+06	5,33E+06
	10 kV – 1 lamp	6,05E+06	4,22E+05	5,96E+06	5,29E+06	5,46E+06	6,78E+06	6,94E+06
	10 kV – 2 lamps	3,87E+06	2,72E+05	3,87E+06	3,17E+06	3,41E+06	4,30E+06	4,54E+06
	10 kV – 3 lamps	4,18E+06	4,16E+05	4,24E+06	3,21E+06	3,48E+06	4,77E+06	5,11E+06
	10 kV – 4 lamps	8,71E+06	5,13E+05	8,75E+06	7,63E+06	7,81E+06	9,44E+06	9,84E+06
	10 kV – 5 lamps	3,20E+06	3,23E+05	3,22E+06	2,52E+06	2,69E+06	3,73E+06	4,00E+06
	11 kV – 0 lamp	8,63E+06	7,11E+05	8,54E+06	7,22E+06	7,56E+06	9,91E+06	1,05E+07
	11 kV – 1 lamp	6,93E+06	9,95E+05	7,29E+06	4,25E+06	5,06E+06	8,15E+06	8,43E+06
	11 kV – 2 lamps	4,39E+06	5,22E+05	4,50E+06	3,36E+06	3,54E+06	5,11E+06	5,45E+06
	11 kV – 3 lamps	6,54E+06	3,68E+05	6,58E+06	5,54E+06	5,88E+06	7,08E+06	7,27E+06
	11 kV – 4 lamps	5,56E+06	2,99E+05	5,55E+06	4,87E+06	5,11E+06	6,04E+06	6,45E+06
	11 kV – 5 lamps	3,72E+06	4,41E+05	3,71E+06	2,80E+06	3,05E+06	4,47E+06	5,19E+06

S1, (25 m³/h)		Mean	Standard Deviation	Median	Minimum	5th percentile	95th percentile	Maximum
PNC, #/cm³	12 kV – 0 lamp	8,54E+06	1,05E+06	8,36E+06	6,71E+06	7,20E+06	1,07E+07	1,11E+07
	12 kV – 1 lamp	7,83E+06	5,98E+05	7,80E+06	6,59E+06	6,97E+06	8,75E+06	9,61E+06
	12 kV – 2 lamps	6,30E+06	4,64E+05	6,27E+06	5,02E+06	5,60E+06	7,04E+06	7,25E+06
	12 kV – 3 lamps	5,08E+06	3,52E+05	5,11E+06	4,34E+06	4,47E+06	5,62E+06	5,84E+06
	12 kV – 4 lamps	3,62E+06	3,17E+05	3,60E+06	3,00E+06	3,15E+06	4,12E+06	4,38E+06
	12 kV – 5 lamps	4,57E+06	3,86E+05	4,53E+06	3,59E+06	4,02E+06	5,22E+06	5,70E+06
	13 kV – 0 lamp	6,12E+06	6,26E+05	6,10E+06	4,97E+06	5,16E+06	7,14E+06	7,68E+06
	13 kV – 1 lamp	4,62E+06	6,78E+05	4,61E+06	3,28E+06	3,49E+06	5,61E+06	6,03E+06
	13 kV – 2 lamps	5,37E+06	3,25E+05	5,39E+06	4,50E+06	4,88E+06	5,90E+06	6,16E+06
	13 kV – 3 lamps	5,48E+06	4,15E+05	5,53E+06	4,57E+06	4,81E+06	6,12E+06	6,46E+06
	13 kV – 4 lamps	5,88E+06	3,81E+05	5,93E+06	4,90E+06	5,27E+06	6,41E+06	6,71E+06
	13 kV – 5 lamps	3,08E+06	2,83E+05	3,08E+06	2,34E+06	2,59E+06	3,52E+06	3,80E+06
	14 kV – 0 lamp	7,06E+06	5,92E+05	7,02E+06	5,28E+06	6,09E+06	8,15E+06	8,47E+06
	14 kV – 1 lamp	7,53E+06	7,02E+05	7,60E+06	6,10E+06	6,41E+06	8,53E+06	9,44E+06
	14 kV – 2 lamps	4,00E+06	3,36E+05	3,95E+06	3,33E+06	3,52E+06	4,64E+06	4,77E+06
	14 kV – 3 lamps	3,70E+03	3,48E+02	3,68E+03	3,07E+03	3,18E+03	4,37E+03	4,52E+03
	14 kV – 4 lamps	4,27E+06	2,97E+05	4,27E+06	3,68E+06	3,81E+06	4,77E+06	4,97E+06
	14 kV – 5 lamps	4,66E+06	4,57E+05	4,66E+06	3,58E+06	4,00E+06	5,40E+06	5,95E+06

Descriptive statistics were performed for the visualization and analysis of particle number concentration (PNC). The mean is the arithmetic average of the measured values, the median and the mean were chosen to be the central tendency measurements, and standard deviation, minimum, and maximum values were utilized for the indicators of data variability. Minimum and Maximum relative particle number concentration represented the lowest and highest concentration in the data

set, and standard deviation illustrated how relative the particle number concentration was distributed around the mean value obtained for each variable.

The mean particle number concentration ranged from $3,08E+06$ #/cm^3 to $8,71E+06$ #/cm^3, depending on the parameter chosen in the S1 experiment. The highest mean ($8,71E+06$ #/cm^3) was recorded in the experiment using the parameters of 4 lamps and 10 kV, and the lowest mean ($3,08E+06$ #/cm^3) was recorded in 5 UVC lamps and 13 kV. The results of the medians exhibit outcomes comparable to those of the mean. The constants in this experiment were temperature, relative humidity, and NTP power.

Table 7. Descriptive statistics of sampling point S2

S2 (25 m³/h)		Mean	Standard Deviation	Median	Minimum	5th percentile	95th percentile	Maximum
	10 kV – 0 lamp	2,41E+06	5,67E+04	2,41E+06	2,27E+06	2,31E+06	2,49E+06	2,50E+06
	10 kV – 1 lamp	3,37E+06	5,07E+04	3,37E+06	3,22E+06	3,25E+06	3,44E+06	3,46E+06
	10 kV – 2 lamps	2,51E+06	5,48E+04	2,51E+06	2,39E+06	2,42E+06	2,60E+06	2,65E+06
	10 kV – 3 lamps	2,81E+06	6,52E+04	2,82E+06	2,68E+06	2,70E+06	2,91E+06	2,97E+06
	10 kV – 4 lamps	4,98E+06	8,68E+04	4,99E+06	4,72E+06	4,86E+06	5,10E+06	5,17E+06
	10 kV – 5 lamps	2,04E+06	3,46E+04	2,04E+06	1,97E+06	1,99E+06	2,11E+06	2,12E+06
	11 kV – 0 lamp	2,58E+06	5,87E+04	2,59E+06	2,42E+06	2,48E+06	2,67E+06	2,69E+06
PNC, #/cm³	11 kV – 1 lamp	3,28E+06	1,31E+05	3,33E+06	2,78E+06	3,11E+06	3,40E+06	3,43E+06
	11 kV – 2 lamps	3,31E+06	8,26E+04	3,32E+06	3,09E+06	3,16E+06	3,43E+06	3,48E+06
	11 kV – 3 lamps	3,87E+06	6,41E+04	3,87E+06	3,74E+06	3,76E+06	3,97E+06	4,02E+06
	11 kV – 4 lamps	3,65E+06	5,61E+04	3,65E+06	3,55E+06	3,58E+06	3,76E+06	3,77E+06
	11 kV – 5 lamps	2,60E+06	6,60E+04	2,61E+06	2,48E+06	2,48E+06	2,71E+06	2,73E+06
	12 kV – 0 lamp	1,86E+06	9,29E+04	1,85E+06	1,70E+06	1,72E+06	2,00E+06	2,01E+06
	12 kV – 1 lamp	2,58E+06	8,00E+04	2,58E+06	2,43E+06	2,46E+06	2,71E+06	2,74E+06
	12 kV – 2 lamps	3,17E+06	6,82E+04	3,17E+06	3,02E+06	3,07E+06	3,28E+06	3,30E+06

S2 (25 m³/h)		Mean	Standard Deviation	Median	Minimum	5th percentile	95th percentile	Maximum
PNC, #/cm³	12 kV – 3 lamps	2,23E+06	4,98E+04	2,23E+06	2,13E+06	2,16E+06	2,32E+06	2,33E+06
	12 kV – 4 lamps	2,44E+06	5,23E+04	2,45E+06	2,32E+06	2,35E+06	2,52E+06	2,54E+06
	12 kV – 5 lamps	1,87E+06	6,95E+04	1,87E+06	1,73E+06	1,75E+06	1,97E+06	2,03E+06
	13 kV – 0 lamp	1,47E+06	5,07E+04	1,48E+06	1,33E+06	1,37E+06	1,53E+06	1,54E+06
	13 kV – 1 lamp	1,50E+06	2,15E+04	1,51E+06	1,44E+06	1,47E+06	1,53E+06	1,54E+06
	13 kV – 2 lamps	2,01E+06	6,59E+04	2,02E+06	1,88E+06	1,89E+06	2,11E+06	2,16E+06
	13 kV – 3 lamps	2,45E+06	5,97E+04	2,45E+06	2,34E+06	2,36E+06	2,55E+06	2,59E+06
	13 kV – 4 lamps	2,51E+06	4,53E+04	2,52E+06	2,40E+06	2,43E+06	2,57E+06	2,58E+06
	13 kV – 5 lamps	1,24E+06	6,02E+04	1,25E+06	1,11E+06	1,14E+06	1,32E+06	1,34E+06
	14 kV – 0 lamp	1,97E+06	5,22E+04	1,97E+06	1,82E+06	1,89E+06	2,05E+06	2,07E+06
	14 kV – 1 lamp	1,79E+06	3,76E+04	1,78E+06	1,72E+06	1,72E+06	1,84E+06	1,85E+06
	14 kV – 2 lamps	1,48E+06	4,50E+04	1,48E+06	1,40E+06	1,42E+06	1,56E+06	1,57E+06
	14 kV – 3 lamps	2,02E+06	4,23E+04	2,01E+06	1,93E+06	1,95E+06	2,08E+06	2,12E+06
	14 kV – 4 lamps	1,58E+06	4,26E+04	1,58E+06	1,49E+06	1,53E+06	1,65E+06	1,68E+06
	14 kV – 5 lamps	1,21E+06	1,95E+04	1,21E+06	1,17E+06	1,18E+06	1,24E+06	1,25E+06

Table 7 shows that the mean in the cases with 10 kV and 4 UVC lamps had the highest mean (4,98E+06 #/cm³), and the 14 kV 5 UVC lamps had the lowest mean (1,21E+06 #/cm³) during the S2 sampling experiment. The mean in S2 varied from 1,21E+06 #/cm³ to 4,98E+06 #/cm³. Medians of PNC showed similar results to the mean. The standard deviation appeared to have lower values and varied from 1,95E+04 #/cm³ to 9,29E+04 #/cm³ according to the parameters chosen.

Table 8. Descriptive statistics of sampling point S3

S3 (25 m³/h)		Mean	Standard Deviation	Median	Minimum	5th percentile	95th percentile	Maximum
PNC, #/cm³	10 kV – 0 lamp	2,63E+03	5,74E+02	2,80E+03	9,25E+02	1,37E+03	3,25E+03	3,44E+03
	10 kV – 1 lamp	3,78E+03	7,68E+02	3,70E+03	2,57E+03	2,68E+03	4,92E+03	5,65E+03
	10 kV – 2 lamps	5,05E+03	3,90E+02	5,06E+03	4,30E+03	4,46E+03	5,54E+03	5,95E+03
	10 kV – 3 lamps	7,59E+03	1,29E+03	7,87E+03	5,01E+03	5,22E+03	9,20E+03	9,71E+03
	10 kV – 4 lamps	1,22E+04	2,09E+03	1,26E+04	7,47E+03	8,09E+03	1,56E+04	1,65E+04
	10 kV – 5 lamps	7,67E+03	1,60E+03	7,77E+03	4,37E+03	4,96E+03	1,04E+04	1,06E+04
	11 kV – 0 lamp	6,64E+03	1,96E+03	6,71E+03	3,97E+03	4,11E+03	9,62E+03	1,05E+04
	11 kV – 1 lamp	6,14E+03	1,47E+03	6,02E+03	2,38E+03	3,57E+03	8,34E+03	9,07E+03
	11 kV – 2 lamps	8,25E+03	1,46E+03	8,62E+03	5,64E+03	5,76E+03	1,04E+04	1,09E+04
	11 kV – 3 lamps	5,63E+03	1,06E+03	5,38E+03	3,36E+03	4,31E+03	7,73E+03	8,05E+03
	11 kV – 4 lamps	9,66E+03	1,40E+03	9,85E+03	5,22E+03	6,32E+03	1,13E+04	1,18E+04
	11 kV – 5 lamps	2,65E+03	3,58E+02	2,58E+03	2,11E+03	2,19E+03	3,33E+03	3,76E+03
	12 kV – 0 lamp	3,02E+03	7,33E+02	2,76E+03	2,20E+03	2,32E+03	4,52E+03	5,44E+03
	12 kV – 1 lamp	3,09E+03	6,59E+02	3,09E+03	1,51E+03	1,91E+03	4,15E+03	4,42E+03
	12 kV – 2 lamps	7,33E+03	1,03E+03	7,41E+03	4,73E+03	5,50E+03	8,89E+03	9,30E+03
	12 kV – 3 lamps	4,38E+03	8,44E+02	4,37E+03	2,55E+03	3,03E+03	5,88E+03	5,95E+03
	12 kV – 4 lamps	4,39E+03	8,53E+02	4,43E+03	3,21E+03	3,30E+03	5,71E+03	5,82E+03
	12 kV – 5 lamps	2,19E+03	6,82E+02	2,13E+03	1,04E+03	1,17E+03	3,30E+03	3,46E+03
	13 kV – 0 lamp	2,10E+03	4,31E+02	2,09E+03	1,23E+03	1,36E+03	2,78E+03	3,05E+03
	13 kV – 1 lamp	3,62E+03	7,25E+02	3,61E+03	2,19E+03	2,50E+03	4,90E+03	5,73E+03

S3 (25 m³/h)		Mean	Standard Deviation	Median	Minimum	5th percentile	95th percentile	Maximum
PNC, #/cm³	13 kV – 2 lamps	2,82E+03	6,23E+02	2,71E+03	1,75E+03	1,83E+03	4,00E+03	4,04E+03
	13 kV – 3 lamps	7,29E+03	1,12E+03	7,33E+03	4,64E+03	5,27E+03	9,29E+03	9,93E+03
	13 kV – 4 lamps	7,14E+03	1,91E+03	7,24E+03	3,29E+03	3,70E+03	1,02E+04	1,11E+04
	13 kV – 5 lamps	2,67E+03	6,60E+02	2,47E+03	1,92E+03	1,99E+03	3,88E+03	4,37E+03
	14 kV – 0 lamp	4,79E+03	1,64E+03	4,67E+03	2,54E+03	2,68E+03	7,59E+03	8,46E+03
	14 kV – 1 lamp	4,68E+03	1,65E+03	4,71E+03	1,96E+03	2,12E+03	7,67E+03	8,22E+03
	14 kV – 2 lamps	3,70E+03	3,48E+02	3,68E+03	3,07E+03	3,18E+03	4,37E+03	4,52E+03
	14 kV – 3 lamps	7,84E+03	7,43E+02	8,03E+03	5,79E+03	6,52E+03	8,77E+03	9,09E+03
	14 kV – 4 lamps	4,45E+03	6,10E+02	4,59E+03	2,98E+03	3,22E+03	5,26E+03	5,31E+03
	14 kV – 5 lamps	3,08E+03	8,50E+02	3,01E+03	1,58E+03	1,98E+03	5,08E+03	5,59E+03

In S3 (Table 8), the mean concentration of total particle number varied from 2,10E+03 #/cm³ to 1,22E+04 #/cm³ depending on the parameter to be modified, the highest at 11 kV 4 lamps and the lowest at 13 kV 0 lamp. Medians showed a similar tendency. The standard deviation in all cases had small values ranging from 3,48E+02 #/cm³ to 2,09E+03 #/cm³.

3.2. Particle size distribution

Six graphs of the particle size distribution (PSD) as a by-product of the VOCs decomposition corresponding to the modified parameters of the UVC lamps are shown below. PSD graphs in S1 show the size distribution of the initial aerosol particles generated in the NTP reactor. The smallest particle had the highest concentration; as the particle size increased, the concentration decreased.

At point S2, the particles located under a bipolar ionizer were exposed to UVC radiation and bipolar ionization, the submicron particles then agglomerated, and the total concentration and small particles concentration decreased. An increase in the concentration of larger particles has been observed in the range of 0,1 to 0,3 micrometers. In some of the S2 graphs, the concentration increased in channels > 0,1, explained by smaller particle agglomeration and the formation of larger particles. The S3 curves were represented as the molecular concentration of the particles after ESP. The particle number concentration decreased intensely compared to the values of the S2 curve.
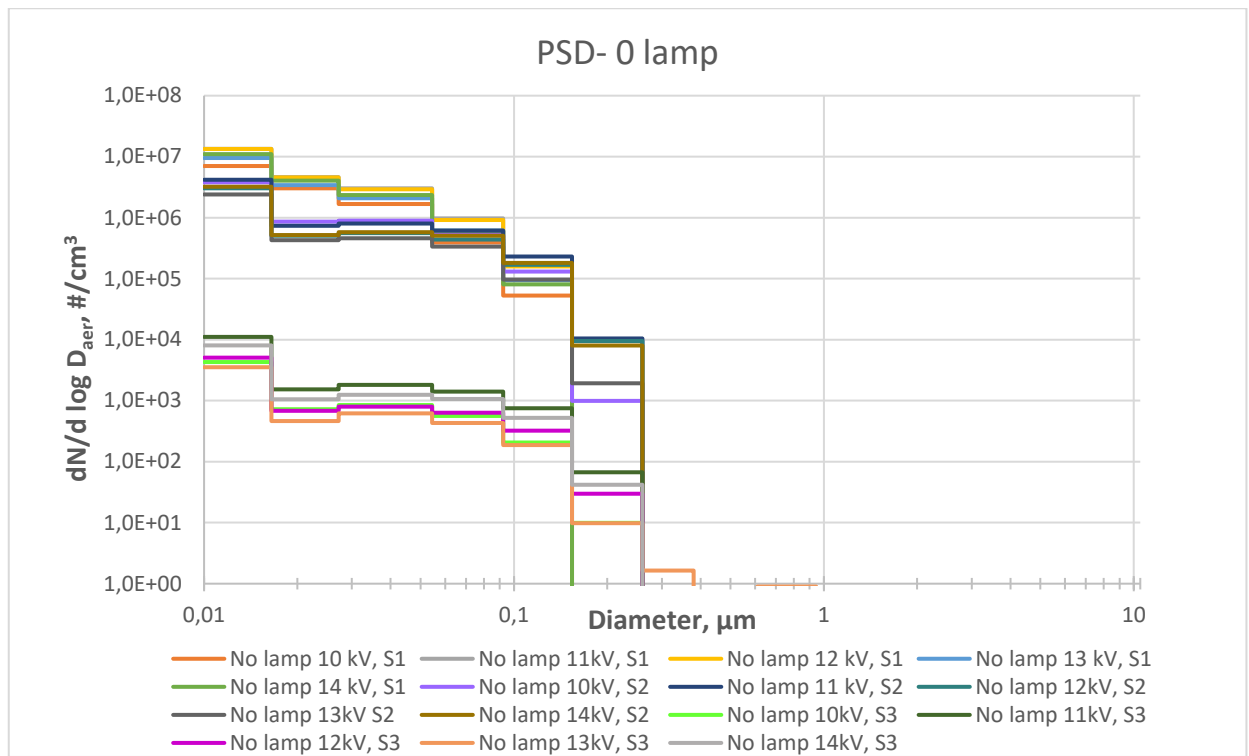
Fig. 16. Particle size distribution graph without UVC lamps

In Fig. 16, the observed levels of particle concentration varied among the investigated data set of the experiment. The particles were in the sub-micrometer size range (range up to 1 μm) and were described that the concentration of particles after NTP in S1 generally fluctuates between 1,34E+07 – 7,06E+06 #/cm^3, and the diameter of the particles formed was around 0,01– 0,02 μm.

When observing that the diameter of aerosol increases, their particle number concentration decreases, and the same tendency is seen for all sampling points. The maximum concentration of particles reached was 1,34E+07 #/cm^3 due to the influence of the nucleation of the heavy molecular cluster in the formation of aerosols.

The particle growth process was generally favorable for the overall removal of the contaminant since larger aerosol particles can be easier to suspend. The sampling point S2, introduced a bipolar ionizer to facilitate the agglomeration of aerosol particles by expanding the size and decreasing the concentration of particles. The PNC of S2 was quite similar independently to S1 of the modification of power values. In bipolar ionization, the airflow is divided by a positive charger generator and a negative one after both airflows are mixed in the reaction chamber, with an opposite charger particle agglomerate. The stage of electrostatic precipitator (ESP) certified the removal of particles efficiency to the outdoor air, and it is shown in the graph that the particle concentration decreased in favor of the removal of particles.
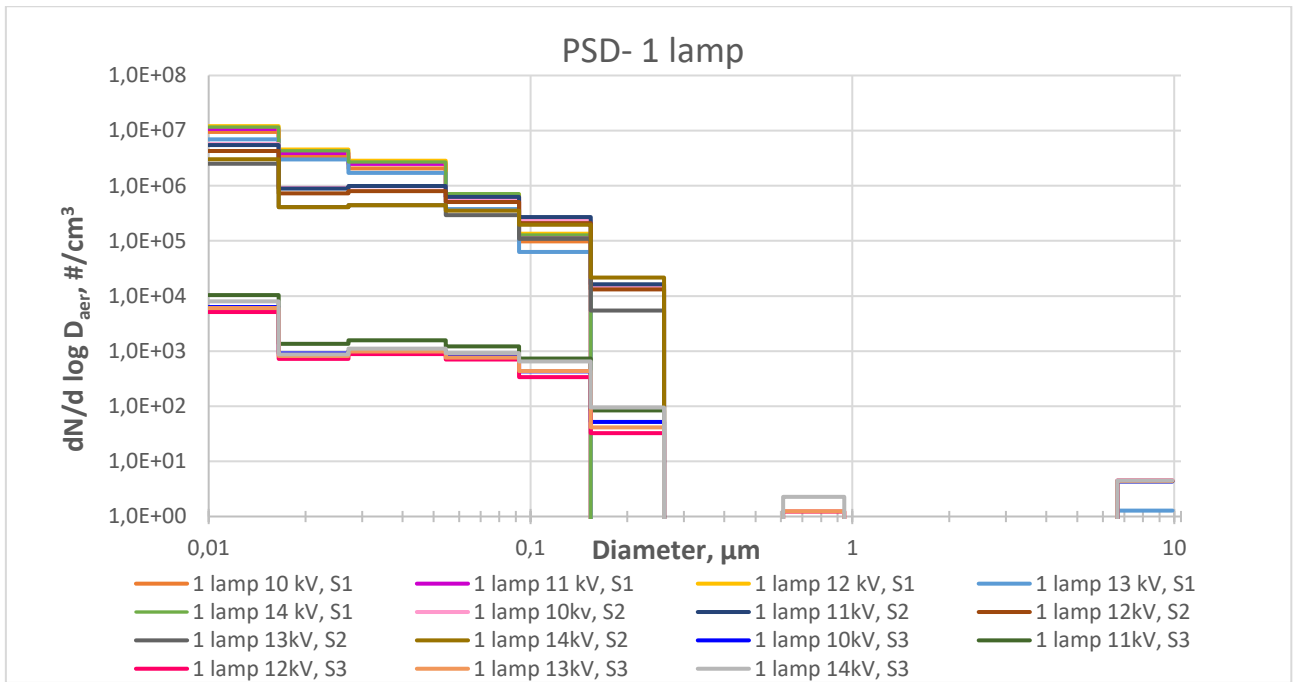
41

Fig. 17. Particle size distribution using 1 UVC lamp in the experiment

Fig. 17 shows the particle size distribution between the concentration and diameter of the aerosols at different sampling points S1, S2, and S3. The majority of the particles were in the submicron size range. The diameter of the aerosol particles in the device at the measurement points S1, S2, and S3 was analyzed in 15 fractions and ranged from 0,01 to 9,88 μm.

The aerosols generated in the graph presented in Fig. 17 contain small fraction particles, and the detection of particles in a size of 9,88 μm was observed. In the data analyzed the highest particle size of 0,01 μm was found in 1,20E+07 #/cm³ at 12kV were observed. The same trend of increasing aerodynamic diameter and decreasing particle concentration was observed.
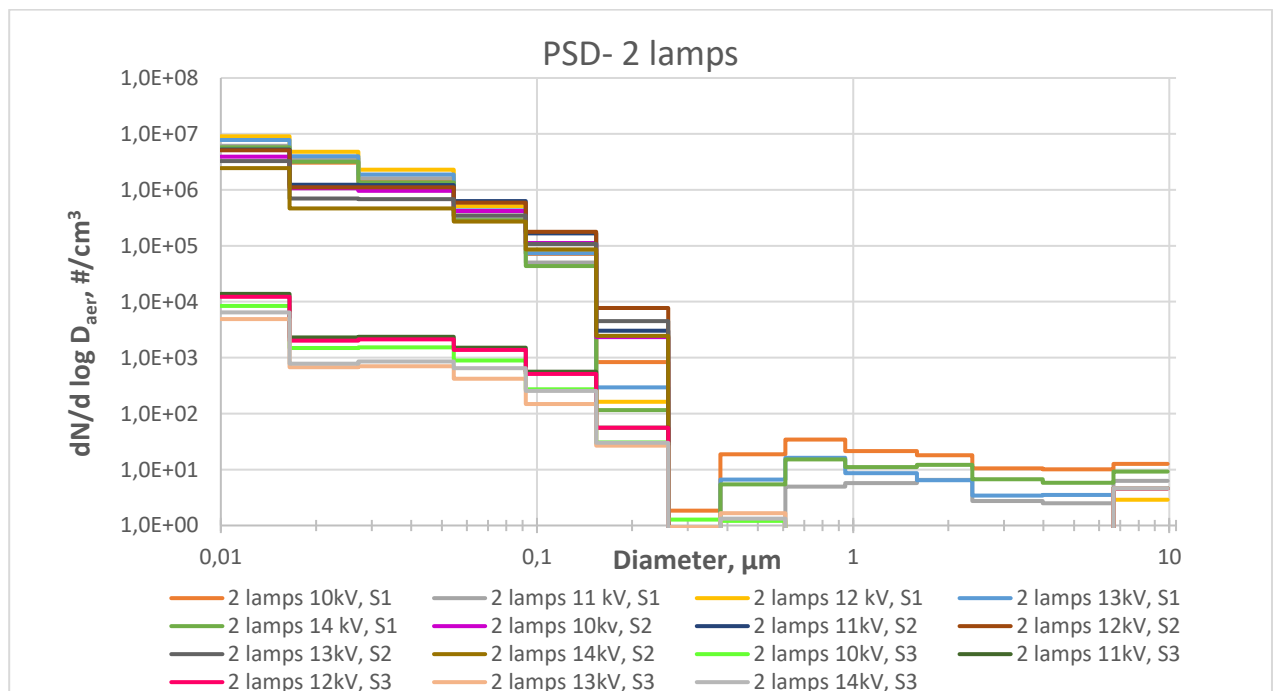
Fig. 18. Particle size distribution using 2 UVC lamps

In Fig. 18, according to the results in the graph, the aerodynamic diameter ranged from 0,01 to 9,88 μm. The particle size distribution followed the trend as Fig. 16 and Fig. 17. The size distribution of the generated particles was greater than one μm.
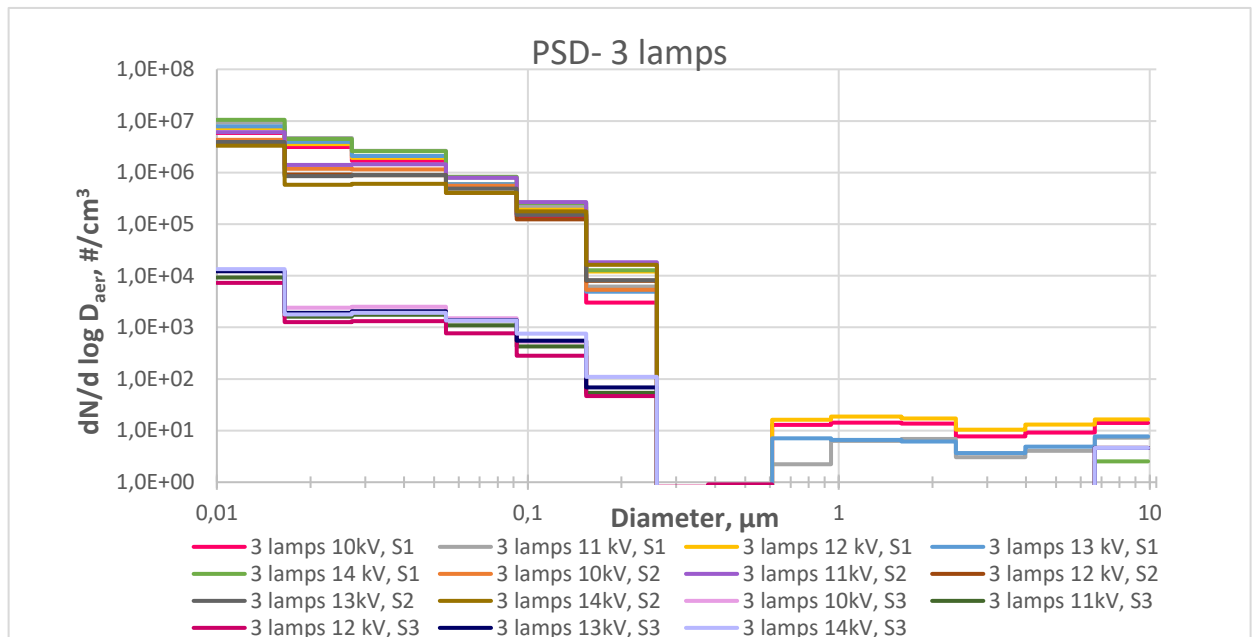

Fig. 19. Particle size distribution using 3 UVC lamps in the experiment

Based on PNC, the particle size distribution showed size ranges from 0,01 to 9,88 μm, occupied by fine and coarse particle fractions.
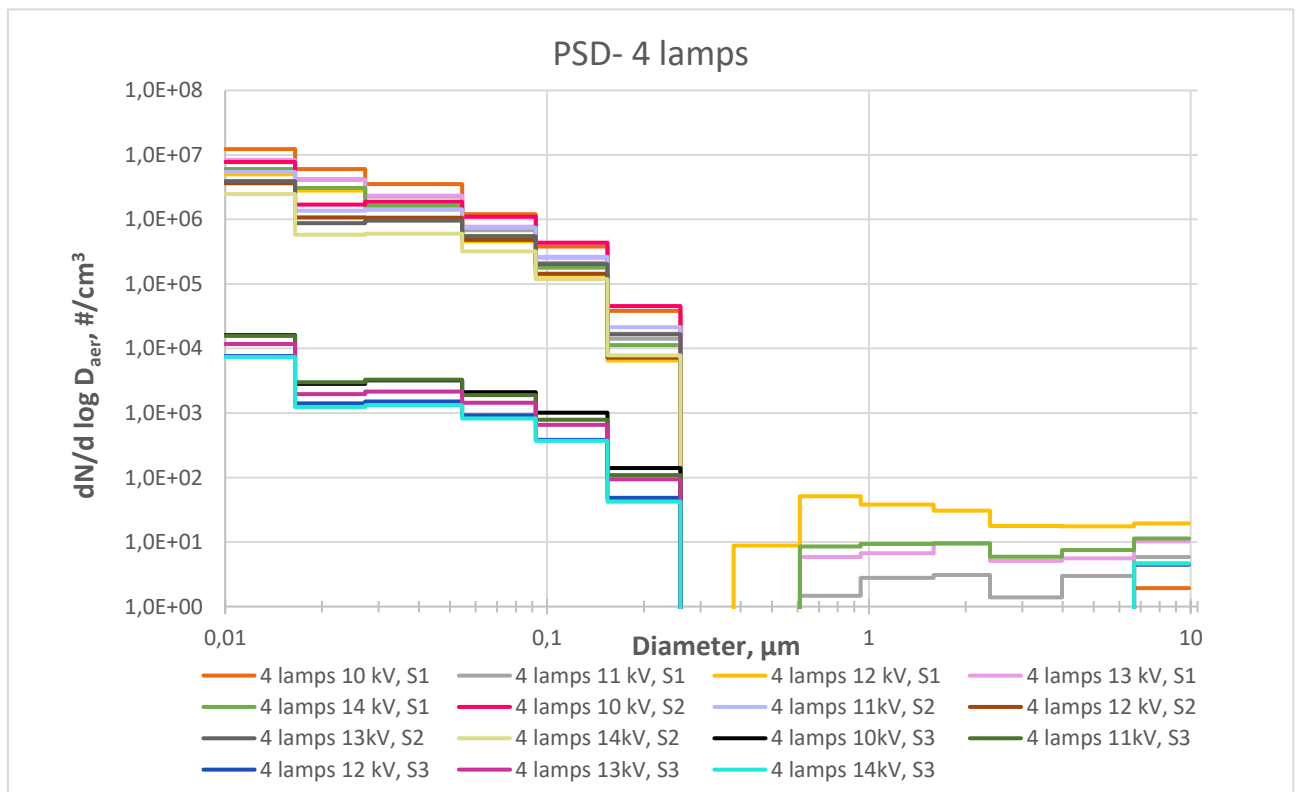

Fig. 20. Particle size distribution using 4 UVC lamps in the experiment

43

The analysis of differences in particle size distributions unveiled the transformation process in aerodynamic size of the aerosol, which followed nucleation, growth, and coagulation. The graph of the size distribution of observed particles was on a logarithmic scale to fit the measurement data. The different colors of the curves represent several experiments on the sampling location and power of the bipolar ionizer. The total particle concentration curve from the size distribution was in the order of units of particles per cm^3.

The 15 curves perform a similar trend, and all gradually decrease. The highest concentration was 13 kV at the S1 sampling point with 0,01 μm, and the lowest concentration was 10 kV, although the largest aerodynamic diameter size (9,88 μm).
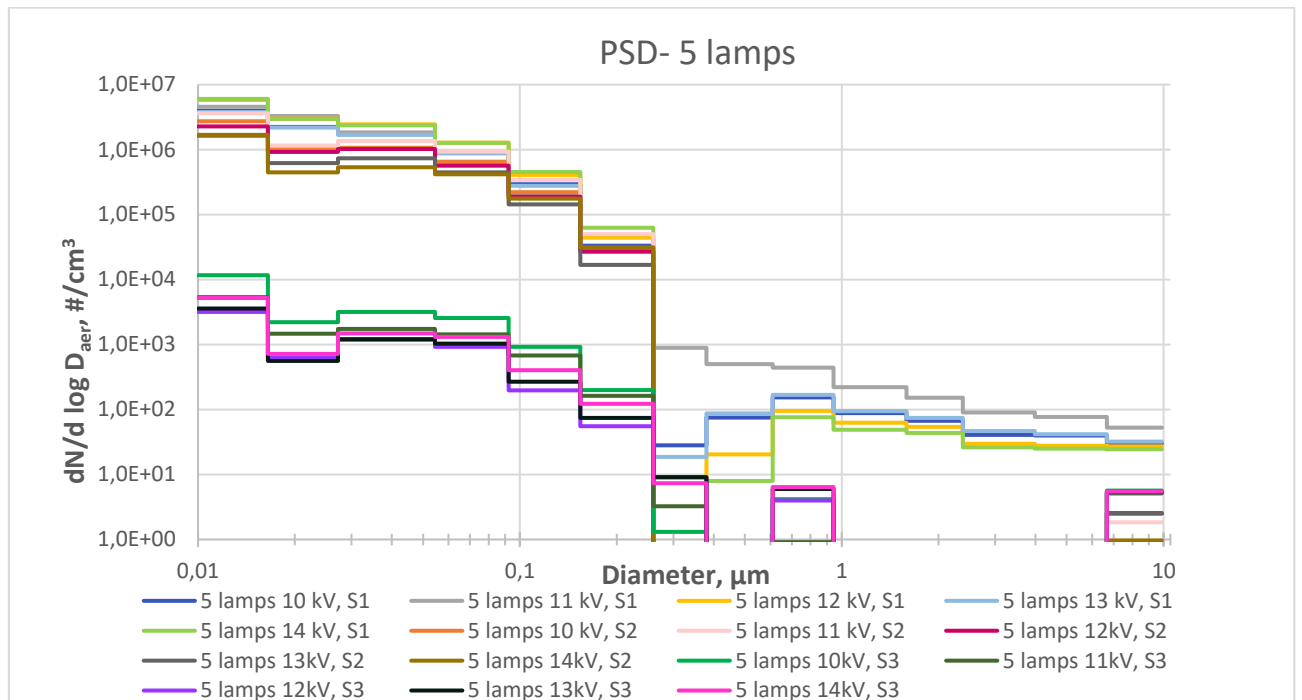

Fig. 21. Particle size distribution using 5 UVC lamps in the experiment

Based on the particle number concentration, the size distribution graph demonstrated that the particles were in the submicron size range, and after NTP, the particle size increased while decreasing its concentration. The decrease in PSD could perhaps be indicated by many factors, such as the dispersion of particles in each stage and partial evaporation of aerosol particles to the gaseous phase, and the deposition of aerosol particles in the surrounding surfaces.

Retention time is shown below in Table 9.

Table 9. Retention time

Purified air flow rate, m^3/h	25
Retention time in the zone from NTP to electrostatic precipitator, sec	128

The aerosol number concentration with respect to the retention time of the NTP to the electrostatic precipitator indicated that aerosols were being removed during the formation process due to the decomposition of VOCs according to the stages of the device. When VOCs decomposed, the number of concentrations decreased.

3.3. Total suspended particles

Six graphs evaluated the total suspended particles in each sampling location of S1, S2, and S3 according to the number of UVC lamps parameter observed in Fig. 22, Fig. 23, Fig. 24, Fig. 25, Fig. 26, and Fig. 27.
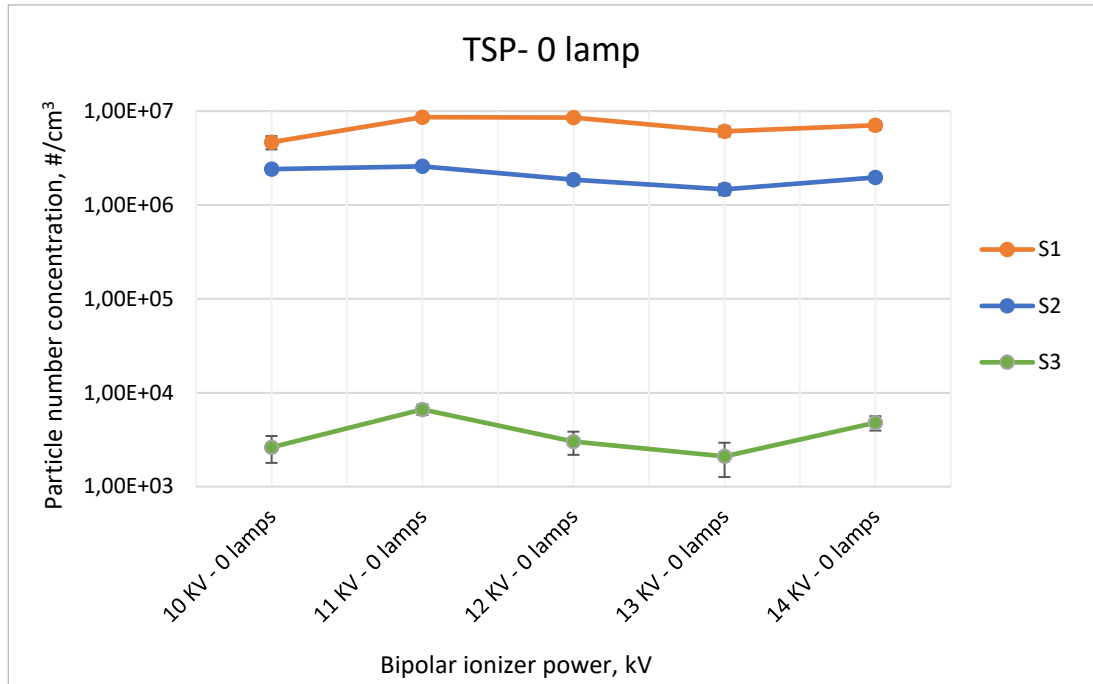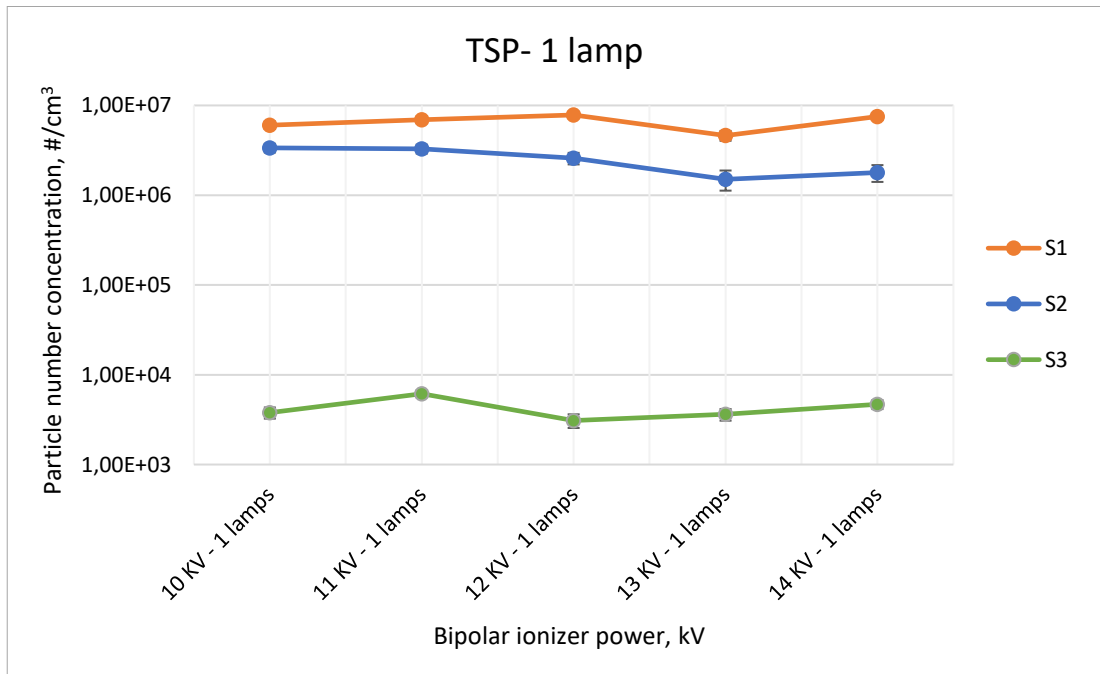

Fig. 22. TSP using no UVC lamps

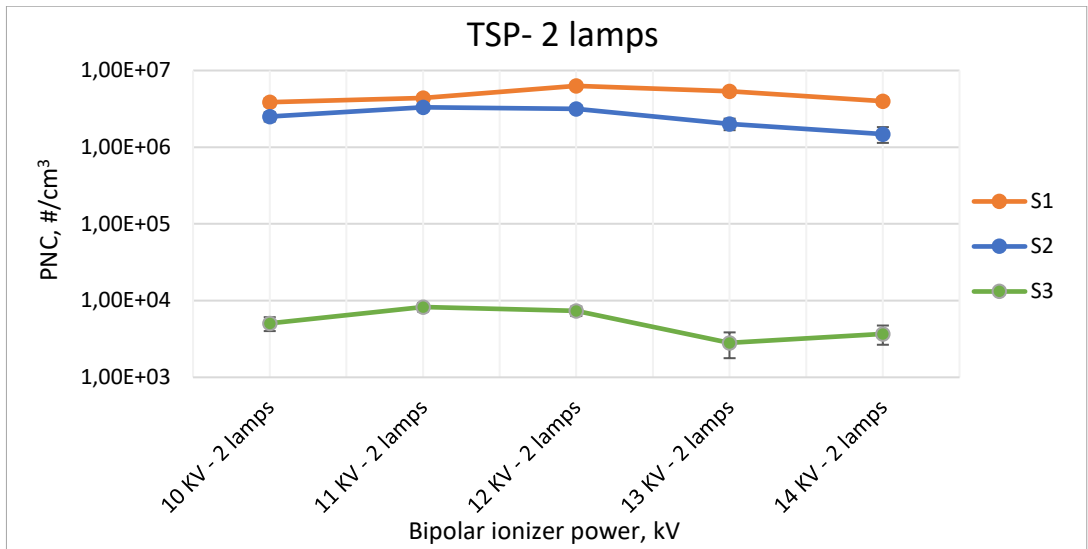**Fig. 23.** TSP using 1 UVC lamp in the experiment

Fig. 24. TSP using 2 UVC lamps in the experiment
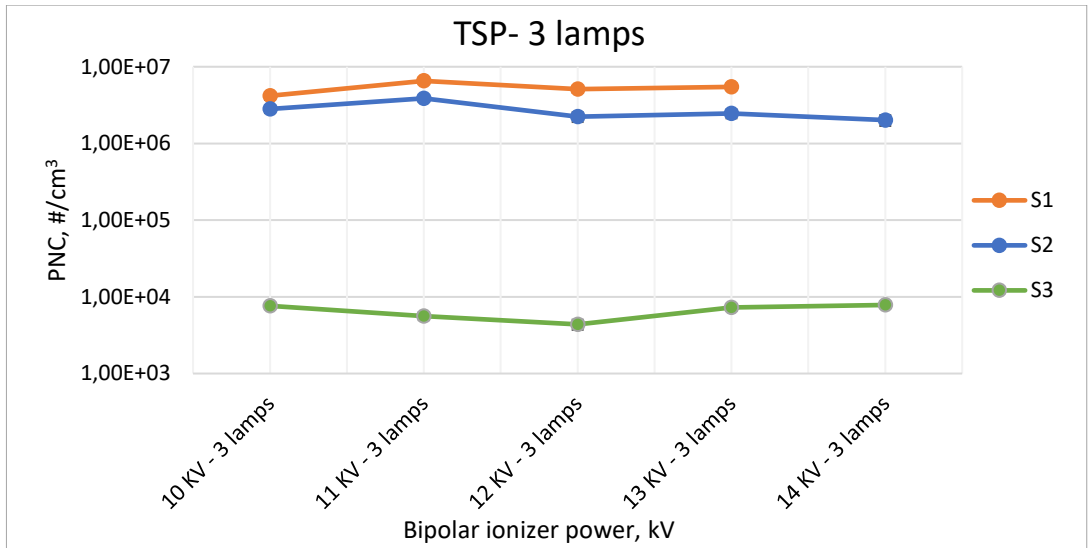

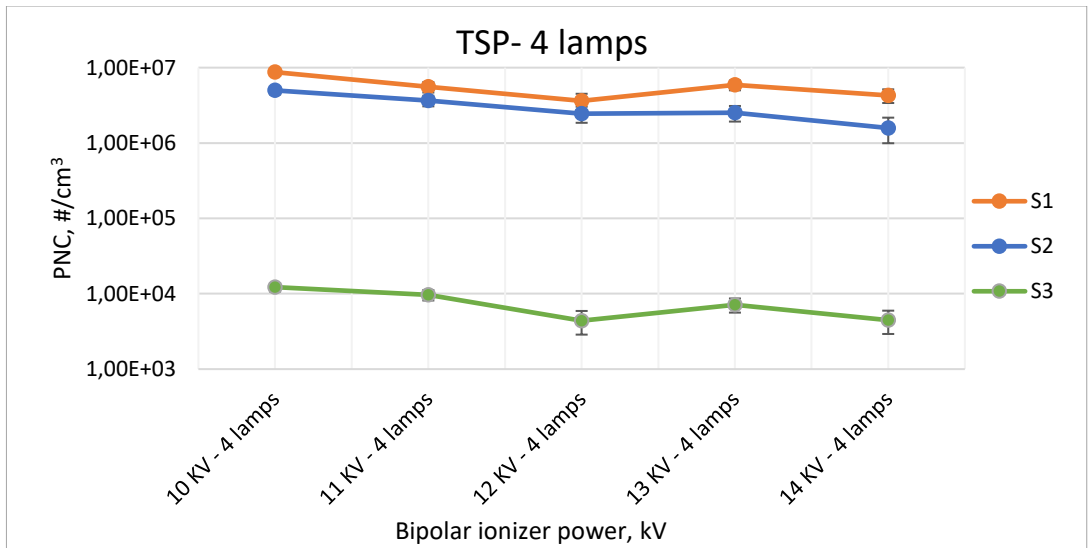**Fig. 25.** TSP using 3 UVC lamps in the experiment

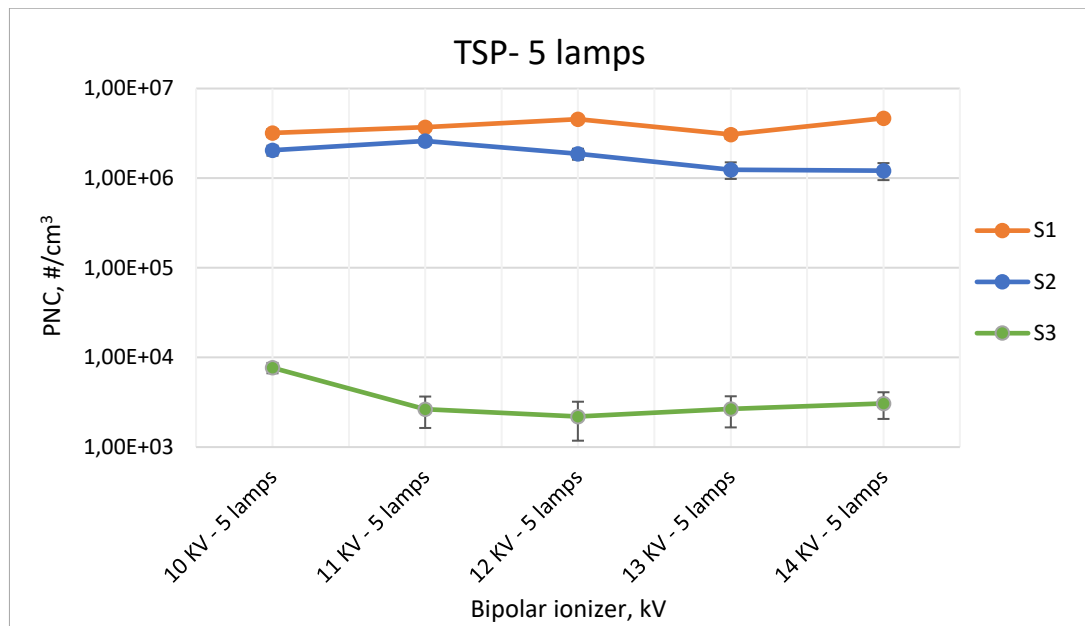**Fig. 26.** TSP using 4 UVC lamps in the experiment

Fig. 27. TSP using 5 UVC lamps in the experiment

Six graphs of TSP noticed that the highest concentrations were at sampling point S1. At sampling point S2, the concentration was reduced and S3 showed significantly lower concentrations. Throughout the study, the trend remains. At the S1 sampling point, the plasma from the NTP reactor converted organic compounds into particles. In addition, many smaller particles were formed. At S2, the particles were affected by bipolar ionization, and there it was agglomerated, and as a result, their number decreased. At the S3 sampling point, the electrostatic precipitator captured particles, and only the residual concentration remained after passing through the ESP.

Observing the curves of S2 and S3 in the above graphs separately at 10 kV and 14 kV, the concentration values did not differ much, and the values were similar when the number of UVC lamps changed. No trends were observed. This led to the conclusion that the number of UVC lamps did not affect aerosol particle concentration.

The TSP graphs of the S3 curves from 10 to 14 kV were analyzed, and their curves did not show a decrease when comparing all the TSP graphs in the S3 sampling point from 0 to 5 lamps. The concentration varied little and there was no trend when analyzing the curves. This concluded that bipolar ionizer voltage within the limits and the number of UVC lamps did not affect the residual concentration of aerosol particles.

3.4. Inferential Statistics analysis

The mean comparison was employed to show statistical differences between various experimental situations. The choice of the test as parametric or non-parametric was based on the distribution of the data. It was necessary to identify if data follow or do not follow a normal distribution and, in this experiment, it did not follow a normal distribution, and to compare the mean difference between the studies, a non-parametric test was employed. The level of significance utilized was 0,05 in this experiment. The t-test was performed in Excel, while the Mann-Whitney U test was performed in SPSS. Table 10 shows the t-test: paired two samples for means in S1.

Table 10. t-test: Paired Two Sample for Means in S1

S1	t-Test: Paired Two Sample for Means		
		Variable 1	*Variable 2*
	Mean	5112824	4586564
	Variance	4,02E+12	7,24E+12
	Observations	6	6
	Pearson Correlation	0,199335	
	Hypothesized Mean Difference	0	
	df	5	
	t Stat	0,427131	
	P(T<=t) one-tail	0,343526	
	t Critical one-tail	2,015048	
	P(T<=t) two-tail	0,687052	
	t Critical two-tail	2,570582	

Table 10 performed the t-Test for S1. The p-value was higher than 0,05, with a p-value of 0,34, ensuring that it was not a statistically significant experiment of 10 kV and 14 kV at the S1 sampling point.

Table 11. t-test: Paired Two Sample for Means performed at the S2 sampling point

S2	t-Test: Paired Two Sample for Means		
		Variable 1	*Variable 2*
	Mean	3021262	1674970
	Variance	1,12E+12	9,52E+10
	Observations	6	6
	Pearson Correlation	0,093664	
	Hypothesized Mean Difference	0	
	df	5	
	t Stat	3,067064	
	P(T<=t) one-tail	0,013938	
	t Critical one-tail	2,015048	
	P(T<=t) two-tail	0,027877	
	t Critical two-tail	2,570582	

Table 11 analyzed the t-test at the sampling measurement point S2, and the p-value was less than 0,05, implying that it was statistically significant and contradicted the null hypothesis, showing evidence that the probability of the null hypothesis being less than 5% is correct, in this experiment

the alternative hypothesis was supported. The Mann-Whitney U test was also performed to ensure such a result.

Table 12. t-Test: Paired Two Sample for Means performed at the S3 sampling point

S3	t-Test: Paired Two Sample for Means		
		Variable 1	*Variable 2*
	Mean	6492,956	4754,131
	Variance	11989919	2705744
	Observations	6	6
	Pearson Correlation	0,043126	
	Hypothesized Mean Difference	0	
	df	5	
	t Stat	1,130109	
	P(T<=t) one-tail	0,154855	
	t Critical one-tail	2,015048	
	P(T<=t) two-tail	0,309709	
	t Critical two-tail	2,570582	

In Table 12, the S3 sampling point was tested in a t-Test, and results showed that p>0,05 was considered not to be statistically significant.

A comparison of measurements at different locations in the prototype was plotted using the Mann-Whitney U test. The concentration of aerosol particles generated was statistically significant (p<0,05) between 10 kV and 14 kV of sampling S2. The difference between each S1 and S3 experiment was found to be statistically insignificant (p>0,05) based on the Mann-Whitney U test for the two independent sample tests.

According to the initial idea, it was stated that bipolar ionizer power enhancement (from 10 to 14 kV) should increase the concentration of aerosol particles, however, it did not happen (S1: no significant difference between 10 kV and 14 kV, S2: there is a significant difference, S3: no significant difference), it denies the hypothesis that concentration of generated aerosol particles increased at higher power. On the contrary, the concentrations decreased, and it could be attributed to the occurrence of ultrafine particle agglomeration.

3.5. Particle removal efficiency

Particle removal efficiency was calculated by the particle number concentration data from S2 and S3 sampling points. Table 13 shows data from PNC S2, and Table 14 shows data from PNC S3.

Table 13. Particle number concentration at the S2 sampling point

PNC S2	10 kV	14 kV
0 Lamp	2,41E+06	1,97E+06
1 Lamp	3,37E+06	1,79E+06
2 Lamps	2,51E+06	1,48E+06
3 Lamps	2,81E+06	2,02E+06
4 Lamps	4,98E+06	1,58E+06
5 Lamps	2,04E+06	1,21E+06

Table 14. Particle number concentration at the S3 sampling point

PNC S3	10 kV	14 kV
0 Lamp	2,63E+03	4,79E+03
1 Lamp	3,78E+03	4,68E+03
2 Lamps	5,05E+03	3,70E+03
3 Lamps	7,59E+03	7,84E+03
4 Lamps	1,22E+04	4,45E+03
5 Lamps	7,67E+03	3,08E+03

Particle removal efficiency was calculated by the particle number concentration in S2 minus the particle number concentration in S3 divided by the particle number concentration in S2 multiplied by 100. Table 15 shows the efficiency in particle removal in each lamp referring to 10 kV and 14 kV.

Table 15. Particle removal efficiency

	10 kV	14 kV
0 Lamp	99,89 %	99,76 %
1 Lamp	99,89 %	99,74 %
2 Lamps	99,8 %	99,75 %
3 Lamps	99,73 %	99,61 %
4 Lamps	99,76 %	99,72 %
5 Lamps	99,62 %	99,75 %

Fig. 28 Represented the device efficiency graph, with curves of S2 and S3 sampling points using particle number concentration.
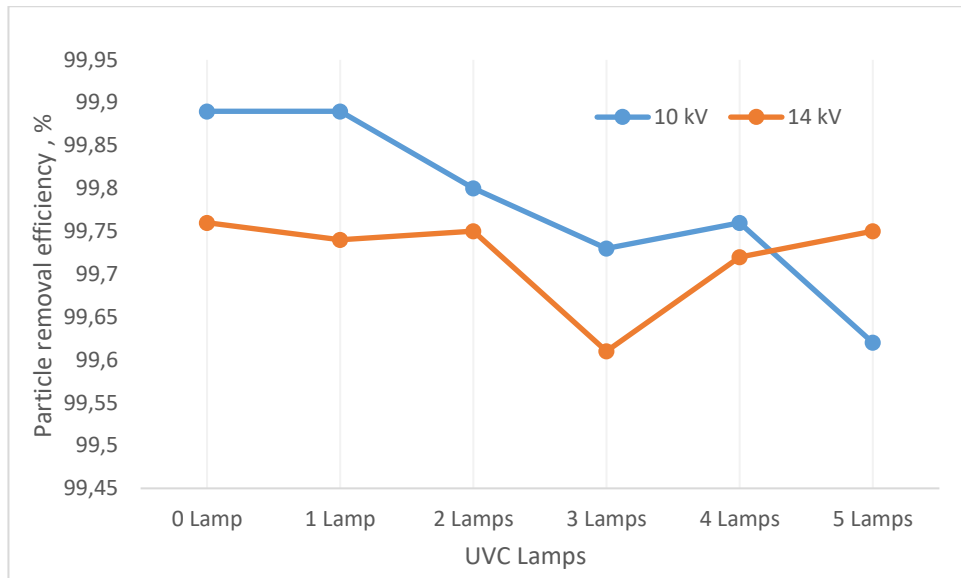
Fig. 28. Particle removal efficiency graph

The particle number concentration decreased with processing time, indicating that aerosols were removed during the formation process; it might be due to the collection of aerosols in the ESP. The experimental results of the particle removal efficiency could be analyzed after S3 (ESP), and the efficiency determination was compared between the PNC of S2 and S3. The device efficiency was calculated by averaging the removal particle efficiency of sampling points S2 and S3. The device had an efficiency of approximately 99,7%.

Fig. 28 shows that when the bipolar ionizer power was at 10 kV, the increased number of lamps led to a decrease in the efficiency of the device, while the number of lamps when the bipolar ionizer power was set at 14 kV did not appear to improve the efficiency of the device and also showed a decrease in efficiency when three lamps were in place.

Based on the test carried out regarding VOC decomposition, the prototype was efficient in airborne particle concentration removal. Furthermore, the reduction in particle number also in the fine fraction was observed during the working prototype, and it had a positive impact on indoor air quality and the smaller particles that enter the respiratory tract that led to the pulmonary alveoli.

51

Conclusions

1. VOCs are hazardous to human health and the environment, having different classifications according to their boiling range. Sources of indoor VOCs come from building materials, smoke, combustion, and others. Approaches are used to mitigate indoor pollution and improve air quality. The complex air cleaner prototype has five stages containing the nucleation of particles (plasmolysis), the coagulation and agglomeration (photolysis and ionization), precipitation of particles (electrostatic precipitation), and the decomposition of residual ozone (ozone destruction).

2. Research plan and methodology for aerosol particle sampling generated in the complex air cleaner prototype was prepared. The experiment had 90 runs containing 30 runs for each sampling point (S1, S2, and S3). The parameters changed were the quantity of UVC lamps (from 0 to 5) and bipolar ionizer power (from 10kV to 14kV), setting constant the flow rate (25 m^3/h), power of NTP and electrostatic precipitator (15kV/-15kV), and concentration of VOCs (5 mg/m^3). The analytical instrument ELPI+ collected in real-time the particle size and concentration and data analyses were performed using Excel and SPSS; t-Test and Mann-Whitney were accomplished.

3. Statistical descriptive statistics were performed for the analysis of PNC. The mean PNC in S1 ranged from 3,08E+06 #/cm^3 to 8,71E+06 #/cm^3, the mean PNC in S2 varied from 1,21E+06 #/cm^3 to 4,98E+06 #/cm^3, while in S3 it ranged from 2,10E+03 #/cm^3 to 1,22E+04 #/cm^3. The PSD graphs were plotted to observe how the particles behaved in relation to their size at each sampling point. The trend of particles was observed in all PSD graphs, and it has shown that the aerodynamic diameter of the particles increased, while their concentration had decreased. The TSP graphs were used to analyse the influence of the variables in the cleaner. No significant trend in aerosol particle concentration was observed changing bipolar ionizer power from 10 to 14 kV in each number of UVC lamps.

4. The complex air cleaner was effective in aerosol particle removal, reaching an average of 99,7% efficiency based on the particle number concentration of S2 and S3. According to the particle removal efficiency graph an increase in UVC lamps did not show an improvement in the device efficiency and an increase of the bipolar ionizer showed a decrease in efficiency.

5. In general, the hypothesis of a positive increase relationship between bipolar ionizer power and the growth of gas-to-particles was rejected, in all three sampling points a positive relationship between the bipolar ionizer power and growth of gas-to-particles was not noticeable, disproving even more in S2 (opposite than the expected) where TSP graph under 14 kV compared to 10 kV was lower. On the other hand, the hypothesis could not be confirmed nor denied because additional experimental studies should be performed while changing different gaseous pollutants (selection of different VOCs) by modifying their concentration levels and airflow rates according to the different combination of parameters that may differently affect on the formation of aerosol particles in the studied system.

List of references

1. ZHANG, Yuanhui. *Indoor air quality engineering*. Online. 1st. CRC Press, 2005. ISBN 9781566706742. Available from: https://www.routledge.com/Indoor-Air-Quality-Engineering/Zhang/p/book/9781566706742 [viewed 2022-03-10]

2. LUENGAS, Angela et al. *A review of indoor air treatment technologies. Reviews in Environmental Science and Biotechnology*. Online. 12 September 2015. Vol. 14, no. 3, p. 499–522. DOI 10.1007/S11157-015-9363-9/FIGURES/7. Available from: https://link.springer.com/article/10.1007/s11157-015-9363-9 [viewed 2022-02-26]

3. VAN TRAN, Vinh et al. Indoor Air Pollution, Related Human Diseases, and Recent Trends in the Control and Improvement of Indoor Air Quality. *International Journal of Environmental Research and Public health*. 2 April 2020. Vol. 17, no. 8. DOI 10.3390/IJERPH17082927.

4. LEVASSEUR, Marie Eve et al. Integrated Management of Residential Indoor Air Quality: A Call for Stakeholders in a Changing Climate. *International Journal of Environmental Research and Public Health*. 1 December 2017. Vol. 14, no. 12. DOI 10.3390/IJERPH14121455.

5. KAUNELIENĖ, Violeta et al. *Indoor air quality in low energy residential buildings in Lithuania. Building and Environment*. 1 November 2016. Vol. 108, p. 63–72. DOI 10.1016/J.BUILDENV.2016.08.018.

6. CIUZAS, Darius et al. *Characterization of indoor aerosol temporal variations for the real-time management of indoor air quality. Atmospheric Environment*. 1 October 2015. Vol. 118, p. 107–117. DOI 10.1016/J.ATMOSENV.2015.07.044.

7. HOMAEIGOHAR, Shahin. Amphiphilic Oxygenated Amorphous Carbon-Graphite Buckypapers with Gas Sensitivity to Polar and Non-Polar VOCs. *Nanomaterials*. Online. 2019. DOI 10.3390/nano9091343. Available from: www.mdpi.com/journal/nanomaterials [viewed 2022-02-27]

8. GUO, Fangfang. *Development of a model for controlling indoor air quality*. PhD thesis. Online. Université de Strasbourg, 2017. Available from: https://tel.archives-ouvertes.fr/tel-01713225 [viewed 2022-02-27]

9. ASILEVI, Prince Junior et al. Indoor air quality improvement and purification by atmospheric pressure Non-Thermal Plasma (NTP). *Scientific Reports 2021 11:1*. Online. 24 November 2021. Vol. 11, no. 1, p. 1–12. DOI 10.1038/s41598-021-02276-1. Available from: https://www.nature.com/articles/s41598-021-02276-1 [viewed 2022-02-22]

10. *Management of Indoor Air Quality by In-Room Air Cleaners and Ventilation*. In : .Online. Barcelona, 2014. Available from: http://wsb14barcelona.org/programme/pdf_poster/P-077.pdf [viewed 2022-02-20]

11. WHO. *Air pollution*. Online. 2022. Available from: https://www.who.int/health-topics/air-pollution#tab=tab_1 [viewed 2022-03-01]

12. SHAW, Stephanie and VAN HEYST, Bill. Performance evaluation of a gaseous pollution control device suitable for in situ heating, ventilation and air conditioning applications. *Clean Technologies and Environmental Policy*. Online. Vol. 1, p. 3. DOI 10.1007/s10098-021-02246-1. Available from: https://doi.org/10.1007/s10098-021-02246-1

13. MAMAGHANI, Alireza Haghighat et al. Photocatalytic oxidation technology for indoor environment air purification: The state-of-the-art. *Applied Catalysis B: Environmental*. 1 April 2017. Vol. 203, p. 247–269. DOI 10.1016/J.APCATB.2016.10.037.

14. LUENGAS, Angela et al. *A review of indoor air treatment technologies. Reviews in Environmental Science and Biotechnology*. Online. 12 September 2015. Vol. 14, no. 3, p. 499–522. DOI 10.1007/S11157-015-9363-9/FIGURES/7. Available from: https://link.springer.com/article/10.1007/s11157-015-9363-9 [viewed 2022-03-01]

15. US EPA. *Introduction to Indoor Air Quality*. Online. December 2021. Available from: https://www.epa.gov/indoor-air-quality-iaq/introduction-indoor-air-quality [viewed 2022-02-16]

16. MANISALIDIS, Ioannis et al. Environmental and Health Impacts of Air Pollution: A Review. *Frontiers in Public Health*. 20 February 2020. Vol. 8, p. 14. DOI 10.3389/FPUBH.2020.00014/BIBTEX.

17. CDC. *Chapter 5: Indoor Air Pollutants and Toxic Materials | Healthy Housing Reference Manual | NCEH. Centers for disease control and prevention*. Online. 1 October 2009. Available from: https://www.cdc.gov/nceh/publications/books/housing/cha05.htm [viewed 2022-02-24].

18. ANDUALEM, Zewudu et al. Indoor bacterial load and its correlation to physical indoor air quality parameters in public primary schools. *Multidisciplinary Respiratory Medicine*. Online. 22 January 2019. Vol. 14, no. 1, p. 1–7. DOI 10.1186/S40248-018-0167-Y/TABLES/6. Available from: https://mrmjournal.biomedcentral.com/articles/10.1186/s40248-018-0167-y [viewed 2022-02-24].

19. BERENJIAN, Aydin et al. Volatile Organic Compounds Removal Methods: A Review. *American Journal of Biochemistry and Biotechnology*. Online. 2012. Vol. 8, no. 4, p. 220–229. DOI 10.3844/ajbbsp.2012.220.229. Available from: http://www.thescipub.com/ajbb.toc [viewed 2022-03-01].

20. VANDENBROUCKE, Arne M. *Abatement of Volatile Organic Compounds by Combined Use of Non-Thermal Plasma and Heterogeneous Catalysis*. Online. 2015. No. 1, p. 371. Available from: https://www.researchgate.net/publication/312493700_Abatement_of_volatile_organic_compounds_by_combined_use_of_non-thermal_plasma_and_heterogeneous_catalysis [viewed 2022-03-01].

21. SONG, Mugeun et al. *Reduction of Volatile Organic Compounds (VOCs) Emissions from Laundry Dry-Cleaning by an Integrated Treatment Process of Condensation and Adsorption*. 2021.

22. DAVID, Elena and NICULESCU, Violeta Carolina. Volatile Organic Compounds (VOCs) as Environmental Pollutants: Occurrence and Mitigation Using Nanomaterials. *International Journal of Environmental Research and Public Health*. Online. 1 December 2021. Vol. 18, no. 24, p. 13147. DOI 10.3390/IJERPH182413147 [viewed 2022-03-02].

23. CANADA.CA. *Volatile organic compounds - Canada.ca*. Online. 29 March 2022. Available from: https://www.canada.ca/en/health-canada/services/air-quality/indoor-air-contaminants/volatile-organic-compounds.html [viewed 2022-03-10].

24. US EPA. *Technical Overview of Volatile Organic Compounds*. Online. Available from: https://www.epa.gov/indoor-air-quality-iaq/technical-overview-volatile-organic-compounds [viewed 2022-03-11].

25. KAMPA, Marilena and CASTANAS, Elias. Human health effects of air pollution. *Environmental Pollution*. 1 January 2008. Vol. 151, no. 2, p. 362–367. DOI 10.1016/J.ENVPOL.2007.06.012.

26. US EPA. *Volatile Organic Compounds' Impact on Indoor Air Quality. O*nline. Available from: https://www.epa.gov/indoor-air-quality-iaq/volatile-organic-compounds-impact-indoor-air-quality [viewed 2022-03-11].

27. SONI, Vipin et al. *Effects of VOCs on Human Health. Energy, Environment, and Sustainability. Air Pollution and Control. Energy, Environment, and Sustainability*. Online. 2018. P. 119–142. DOI 10.1007/978-981-10-7185-0_8. Available from: https://link.springer.com/chapter/10.1007/978-981-10-7185-0_8 [viewed 2022-03-22].

28. LUENGAS, Angela et al. *A review of indoor air treatment technologies.*

DOI <u>10.1007/s11157-015-9363-9</u>.

29. SIEGEL, J. A. Primary and secondary consequences of indoor air cleaners. *Indoor Air*. 2016. Vol. 26, no. 1, p. 88–96. DOI <u>10.1111/ina.12194</u>.

30. WARGOCKI, Pawel. *Filtration and Air Cleaning* . *ASHRAE* .Online. December 2015. Vol. 57, no. 12, p. 70–72. Available from: <u>https://www.proquest.com/openview/e701f609d50c8c6d3daf2a390fd1329a/1?pq-origsite=gscholar&cbl=41118</u> [viewed 2022-03-23].

31. CONDORCHEM ENVITECH. *AIR TREATMENT Solutions and Technologies*. Online. Available from: <u>www.condorchem.com</u> [viewed 2022-02-22]

32. KRUGLY, Edvinas et al. VOC removal from ventilation air by gas-to-particle conversion: Towards the Enhancement of process efficiency. *Building and Environment*. Online. 2022. Vol. 209, no. November 2021, p. 108647. DOI 10.1016/j.buildenv.2021.108647. Available from: <u>https://doi.org/10.1016/j.buildenv.2021.108647</u> [viewed 2021-12-13].

33. KRUGLY, Edvinas et al. Removal of VOCs from wood processing ventilation air by advanced oxidation gas-to-particle prototype system. *Process Safety and Environmental Protection*. Online. 2022. Vol. 161, p. 520–527. DOI 10.1016/j.psep.2022.03.043. Available from: <u>https://doi.org/10.1016/j.psep.2022.03.043</u> [viewed 2022-01-13].

34. BERENJIAN, Aydin et al. Volatile Organic Compounds Removal Methods: A Review. *American Journal of Biochemistry and Biotechnology*. Online. 2012. Vol. 8, no. 4, p. 220–229. DOI 10.3844/ajbbsp.2012.220.229. Available from: <u>http://www.thescipub.com/ajbb.toc</u> [viewed 2022-02-14].

35. QU, Miaomiao et al. Non-thermal plasma coupled with catalysis for VOCs abatement: A review. *Process Safety and Environmental Protection*. 1 September 2021. Vol. 153, p. 139–158. DOI <u>10.1016/J.PSEP.2021.06.028</u>.

36. LOS ALAMOS NATIONAL LABORATORY. *Advanced oxidation and reduction processes in the gas phase using non-thermal plasmas.* New Mexico, 1998.

37. CHOI, Sung Won et al. Photolysis and TiO2 Photocatalytic Treatment under UVC/VUV Irradiation for Simultaneous Degradation of Pesticides and Microorganisms. *Applied Sciences*. Online. 29 June 2020. Vol. 10, no. 13, p. 4493. DOI 10.3390/APP10134493. Available from: <u>https://www.mdpi.com/2076-3417/10/13/4493/htm</u> [viewed 2022-02-15].

38. GURURANI, Prateek et al. Cold plasma technology: advanced and sustainable approach for wastewater treatment. *Environmental Science and Pollution Research*. Online. 1 December 2021. Vol. 28, no. 46, p. 65062–65082. DOI 10.1007/S11356-021-16741-X/TABLES/2. Available from: <u>https://link.springer.com/article/10.1007/s11356-021-16741-x</u> [viewed 2022-03-17].

39. VANDENBROUCKE, Arne M. et al. Non-thermal plasmas for non-catalytic and catalytic VOC abatement. *Journal of Hazardous Materials*. Online. 2011. Vol. 195, no. x, p. 30–54. DOI 10.1016/j.jhazmat.2011.08.060. Available from: <u>http://dx.doi.org/10.1016/j.jhazmat.2011.08.060</u> [viewed 2022-02-18].

40. ASILEVI, Prince Junior et al. Indoor air quality improvement and purification by atmospheric pressure Non-Thermal Plasma (NTP*). Scientific Reports 2021 11:1* [online]. 24 November 2021. Vol. 11, no. 1, p. 1–12. DOI 10.1038/s41598-021-02276-1. Available from: <u>https://www.nature.com/articles/s41598-021-02276-1</u> [viewed 2022-02-14].

41. QU, Miaomiao et al. Non-thermal plasma coupled with catalysis for VOCs abatement: A review. *Process Safety and Environmental Protection*. 1 September 2021. Vol. 153, p. 139–158. DOI <u>10.1016/J.PSEP.2021.06.028</u>.

42. CANADA.CA. *Common air pollutants: volatile organic compounds*. Online. 2013. Available from: <u>https://www.canada.ca/en/environment-climate-change/services/air-pollution/pollutants/common-contaminants/volatile-organic-compounds.html</u> [viewed 2022-04-12].

43. US EPA. *Particulate Matter (PM) Basics*. Online. 2022. Available from: https://www.epa.gov/pm-pollution/particulate-matter-pm-basics#PM [viewed 2022-04-13].

44. ZHANG, Xuming et al. Aerosol formation from styrene removal with an AC/DC streamer corona plasma system in air. *Chemical Engineering Journal*. 1 October 2013. Vol. 232, p. 527–533. DOI 10.1016/J.CEJ.2013.08.009.

45. POSPISILOVA, Veronika et al. Photodegradation of α-Pinene Secondary Organic Aerosol Dominated by Moderately Oxidized Molecules. *Environ. Sci. Technol*. Online. 2021. Vol. 55, p. 6943. DOI 10.1021/acs.est.0c06752. Available from: https://doi.org/10.1021/acs.est.0c06752 [viewed 2023-05-10].

46. MALECHA, Kurtis T and NIZKORODOV, Sergey A. *Photodegradation of Secondary Organic Aerosol Particles as a Source of Small, Oxygenated Volatile Organic Compounds*. Online. 2016. DOI 10.1021/acs.est.6b02313. Available from: https://pubs.acs.org/sharingguidelines [viewed 2022-03-11].

47. HALLQUIST, M. et al. The formation, properties and impact of secondary organic aerosol: Current and emerging issues. *Atmospheric Chemistry and Physics*. 2009. Vol. 9, no. 14, p. 5155–5236. DOI 10.5194/ACP-9-5155-2009.

48. MIRHOSSEINI, Seyed Hamed et al. Analysis of Particulate matter (PM $_{10}$ and PM $_{2.5}$) concentration in Khorramabad city. *International Journal of Environmental Health Engineering*. Online. 2013. Vol. 2, no. 1, p. 3. DOI 10.4103/2277-9183.106635. Available from: https://www.ijehe.org/article.asp?issn=2277-9183;year=2013;volume=2;issue=1;spage=3;epage=3;aulast=Mirhosseini [viewed 2023-05-01]

49. CANADA.CA. *Particulate matter 2.5 and 10*. Online. Available from: https://www.canada.ca/en/environment-climate-change/services/air-pollution/pollutants/common-contaminants/particulate-matter.html [viewed 2023-04-28]

50. GREEN FACTS. *What is Particulate Matter (PM)?*. Online. 2022. Available from: https://www.greenfacts.org/en/particulate-matter-pm/level-3/01-presentation.htm#1p0 [viewed 2023-04-29].

51. EUROPEAN ENVIRONMENT AGENCY. *What is particulate matter and what are its effects on human health?*. Online. Available from: https://www.eea.europa.eu/help/faq/what-is-particulate-matter-and [viewed 2023-04-22].

52. OZONE SOLUTIONS. *How an Ozone Generator Works*. Online. 1 November 2021. Available from: https://ozonesolutions.com/blog/how-an-ozone-generator-works/ [viewed 2023-05-01].

53. PEKÁREK, S. Non-Thermal Plasma Ozone Generation. *Acta Polytechnica*. 2003. Vol. 43, no. 6. DOI 10.14311/498.

54. GEORGE, Adwek et al. *A Review of Non-Thermal Plasma Technology : A novel solution for CO2 conversion and utilization. Renewable and sustainable energy reviews*. Online. 2021. Available from: https://pureadmin.qub.ac.uk/ws/portalfiles/portal/237817617/Final_clean_version.pdf [viewed 2022-02-13].

55. CÉDAT, Bruno et al. Are UV photolysis and UV/H2O2 process efficient to treat estrogens in waters? Chemical and biological assessment at pilot scale. *Water Research*. 2016. Vol. 100, p. 357–366. DOI 10.1016/j.watres.2016.05.040.

56. CHOI, Eureka et al. Formation of Secondary Organic Aerosols by Germicidal Ultraviolet Light. *Environments*. Online. 31 January 2019. Vol. 6, no. 2, p. 17. DOI 10.3390/ENVIRONMENTS6020017. Available from: https://www.mdpi.com/2076-3298/6/2/17/htm [viewed 2022-04-01].

57. LIU, Chao Yun et al. The Study of an Ultraviolet Radiation Technique for Removal of the Indoor Air Volatile Organic Compounds and Bioaerosol. *International Journal of*

Environmental Research and Public Health. 2019. Vol. 16, no. 14. DOI 10.3390/IJERPH16142557.

58. KANG, In-Sun et al. Photolysis and photooxidation of typical gaseous VOCs by UV Irradiation: Removal performance and mechanisms. *Front. Environ. Sci. Eng*. Online. DOI 10.1007/s11783-018-1032-0. Available from: https://doi.org/10.1007/s11783-018-1032-0

59. TRANE TECHNOLOGIES. *A Taxonomy of Air-Cleaning Technologies Featuring Bipolar Ionization.* Online. 2021. Available from: https://www.jp.trane.com/content/dam/Trane/Commercial/global/about-us/wellsphere/Technology Whitepaper - Bipolar Ionization.pdf [viewed 2022-04-02].

60. KIM, Ki Hyun et al. Air ionization as a control technology for off-gas emissions of volatile organic compounds. *Environmental Pollution*. Online. 2017. Vol. 225, p. 729–743. DOI 10.1016/J.ENVPOL.2017.03.026. Available from: https://www.researchgate.net/publication/315667892_Air_ionization_as_a_control_technology_for_off-gas_emissions_of_volatile_organic_compounds [viewed 2022-03-27].

61. US EPA. *Can air cleaning devices that use bipolar ionization, including portable air cleaners and in-duct air cleaners used in HVAC systems, protect me from COVID-19?* .Online. Available from: https://www.epa.gov/coronavirus/can-air-cleaning-devices-use-bipolar-ionization-including-portable-air-cleaners-and [viewed 2022-04-02].

62. KRULL, Bronson et al. *Bipolar Ionization: Understanding the difference between theory and practice*. 2008. Synexis biodefense air and surfaces.

63. CABA. *Bipolar Ionization and its Contribution to Smart and Safe Buildings*. Online. 2021. Available from: www.caba.org

64. ZENG, Yicheng et al. Evaluating a commercially available in-duct bipolar ionization device for pollutant removal and potential byproduct formation. *Building and Environment*. 15 May 2021. Vol. 195, p. 107750. DOI 10.1016/J.BUILDENV.2021.107750.

65. AFSHARI, Alireza et al. Electrostatic Precipitators as an Indoor Air Cleaner-A Literature Review. *Sustainability*. DOI [10.3390/su12218774](10.3390/su12218774).

66. EUROPEAN COMMISION. *Best available technique*. Reference document for common waste gas management and treatment systems in the chemical sector. Online. Available from: https://eippcb.jrc.ec.europa.eu/sites/default/files/2022-03/WGC_Final_Draft_09Mar2022-B-W-Watermark.pdf [viewed 2022-03-09].

67. *Lesson 2 Electrostatic Precipitator Components*. Online. Available from: https://ppcair.com/pdf/EPA Lesson Lesson 2 - Electrostatic Precipitator Components.pdf [viewed 2022-03-05].

68. FLAGAN, Richard C. et al. *Fundamentals of air pollution engineering. The John Zink Hamworthy combustion handbook*. 2nd ed. vol. 1 Fundamentals. 2012. ISBN 9781439839638.

69. LIU, Guoliang et al. *A review of air filtration technologies for sustainable and healthy building ventilation. Sustainable Cities and Society*. 1 July 2017. Vol. 32, p. 375–396. DOI [10.1016/J.SCS.2017.04.011](10.1016/J.SCS.2017.04.011).

70. LI, Wei et al. Mechanism of ozone decomposition on a manganese oxide catalyst. 1. In situ Raman spectroscopy and Ab initio molecular orbital calculations. *Journal of the American Chemical Society*. 1998. Vol. 120, no. 35, p. 9041–9046. DOI [10.1021/ja981441+](10.1021/ja981441+).

71. SEKIGUCHI, Kazuhiko et al. Ozone Catalytic Oxidation of Gaseous Toluene over MnO 2-Based Ozone Decomposition Catalysts Immobilized on a Nonwoven Fabri*c*. *Aerosol and Air Quality Research*. 2017. Vol. 17, p. 2110–2118. DOI 10.4209/aaqr.2017.01.0045.

72. YUB LEE, Jun et al. *Decomposition of gas-phase ozone using natural manganese ore as a catalyst at room temperature*. Third International symposium on air quality management at urban, regional and global scales. 26-30 september 2005. p.1094–1106.

73. RISTIMÄKI, Jyrki et al. On-line measurement of size distribution and effective density of submicron aerosol particles. *Journal of Aerosol Science*. 1 November 2002. Vol. 33, no. 11, p. 1541–1557. DOI 10.1016/S0021-8502(02)00106-4.

74. CHARVET, Augustin et al. *On the Importance of Density in ELPI Data Post-Treatment*. Online. 2 December 2015. Vol. 49, no. 12, p. 1263–1270. DOI 10.1080/02786826.2015.1117568. Available from: https://www-tandfonline-com.ezproxy.ktu.edu/doi/abs/10.1080/02786826.2015.1117568 [viewed 2023-03-05].

75. JÄRVINEN, A. et al. Calibration of the new electrical low pressure impactor (ELPI+). *Journal of Aerosol Science*. 1 March 2014. Vol. 69, p. 150–159. DOI 10.1016/J.JAEROSCI.2013.12.006.

76. MARJAMÄKI, Marko et al. ELPI response and data reduction I: Response functions. *Aerosol Science and Technology*. Online. July 2005. Vol. 39, no. 7, p. 575–582. DOI 10.1080/027868291009189. Available from: https://www.tandfonline.com/action/journalInformation?journalCode=uast20 [viewed 2023-02-04].

77. KESKINEN, J. et al. Electrical low pressure impactor. *Journal of Aerosol Science*. 1992. Vol. 23, no. 4, p. 353–360. DOI 10.1016/0021-8502(92)90004-F.

78. MARJAMÄKI, Marko et al. Performance evaluation of the electrical low-pressure impactor (ELPI). *Journal of Aerosol Science*. 1 February 2000. Vol. 31, no. 2, p. 249–261. DOI 10.1016/S0021-8502(99)00052-X.

79. GRABYS, Tomas. *Jutiklių utiklių naudojimas patalpų oro kokybės valdymui*. Master thesis. Kaunas University of Technology, 2018.

80. KERAITYTĖ, Karolina. *Sumažintos rizikos tabako produktų naudojimo poveikis patalpų oro kokybei.*Master thesis. Kaunas Univeristy of Technology. 2019.

81. AGNE, Kasparaite. *Naujų nikotino turinčių produktų generuojamo aerozolio charakterizavimas ir palyginamasis vertinimas laboratorinio modeliavimo būdu*. Master thesis. Kaunas Univeristy of Technology. 2018.

82. MEŠČERIAKOVAS, Arūnas. *Aerozolio dalelių formavimąsi lemiantys veiksniai ir matavimas neterminės plazmos oro valymo reaktoriuje*. Master thesis. Kaunas University of Technlogy, 2016.

83. PRASAUSKAS, Tadas. Air contamination by particulate matter from processes of building refurbishment and operation. PhD thesis. Kaunas University of Technology, 2014.

84. MEIŠUTOVIČ-AKHTARIEVA, Marija et al. Impacts of exhaled aerosol from the usage of the tobacco heating system to indoor air quality: A chamber study. *Chemosphere*. 2019. Vol. 223, p. 474–482. DOI 10.1016/j.chemosphere.2019.02.095.